

Article

H_{∞} Based Control for Load Mitigation in Wind Turbines

Asier Diaz de Corcuera *, Aron Pujana-Arrese, Jose M. Ezquerro, Edurne Segurola and Joseba Landaluze

IKERLAN-IK4, Arizmendiarreta, 2, E-20500 Arrasate-Mondragon, The Basque Country, Spain;
E-Mails: apujana@ikerlan.es (A.P.-A.); jmezquerro@ikerlan.es (J.M.E.);
mesegurola@ikerlan.es (E.S.); jlandaluze@ikerlan.es (J.L.)

* Author to whom correspondence should be addressed; E-Mail: adiazcorcuera@ikerlan.es;
Tel.: +34-943-712-400; Fax: +34-943-796-944.

Received: 25 January 2012; in revised form: 20 March 2012 / Accepted: 31 March 2012 /

Published: 17 April 2012

Abstract: This article demonstrates a strategy to design multivariable and multi-objective controllers based on the H_{∞} norm reduction applied to a wind turbine. The wind turbine model has been developed in the GH Bladed software and it is based on a 5 MW wind turbine defined in the Upwind European project. The designed control strategy works in the above rated power production zone and performs generator speed control and load reduction on the drive train and tower. In order to do this, two robust H_{∞} MISO (Multi-Input Single-Output) controllers have been developed. These controllers generate collective pitch angle and generator torque set-point values to achieve the imposed control objectives. Linear models obtained in GH Bladed 4.0 are used, but the control design methodology can be used with linear models obtained from any other modelling package. Controllers are designed by setting out a mixed sensitivity problem, where some notch filters are also included in the controller dynamics. The obtained H_{∞} controllers have been validated in GH Bladed and an exhaustive analysis has been carried out to calculate fatigue load reduction on wind turbine components, as well as to analyze load mitigation in some extreme cases. The analysis compares the proposed control strategy based on H_{∞} controllers to a baseline control strategy designed using the classical control methods implemented on the present wind turbines.

Keywords: wind turbine; robust control; multivariable; H_{∞} control; load mitigation

1. Introduction

The continuous increase of the size of wind turbines, due to the demand of higher power production installations, has led to new challenges in the design of the turbines. Moreover, new control strategies are being developed. Today's strategies trend towards being multivariable and multi-objective in order to fulfill the numerous control design specifications. To be more precise, one important specification is to mitigate loads in the turbine components to increase their life time. This can be done through the components mechanical design, the introduction of new materials or by improving the control itself. In addition to this, the behaviour of a wind turbine is non-linear, which implies that the designed control performance has to be robust.

Over the last few years, several modern control techniques used to replace the classical PI controllers (see Section 3) have been developed. These techniques are fuzzy controllers [1], adaptive control strategies [2], linear quadratic controllers [3] like the Disturbance Accommodating Control (DAC) [4] developed by NREL and tested in the CART real wind turbine [5], QFT controllers [6], Linear Parameter Varying (LPV) controllers [7] and controllers based on the H_∞ norm reduction. H_∞ controllers have the capacity for robustness and these controllers are multivariable and multi-objective, so their applications in wind turbine control offer a lot of advantages and they achieve interesting results. One article dealing with this topic [8] shows the design of two controllers based on the H_∞ norm reduction applied to a simple and analytical model of a wind turbine. The first one reduces the loads on the tower with the tower fore-aft acceleration displacement measurement and controls the generator speed reference with a pitch collective control in the above rated zone. The second controller also reduces the loads on the blades with a cyclic pitch controller based on the H_∞ norm reduction. Control strategies using SISO and MISO state-space controllers based on the H_∞ norm are tested and compared in the CART3 experimental wind turbine [9]. In this article, torque controllers are used to damp the drive train mode and the tower side-to-side bending mode.

This article presents the design of two H_∞ MISO (Multi-Input Single-Output) controllers in the above rated zone (see Section 5). These controllers not only control the generator speed and reduce the fore-aft displacements on the tower using a collective pitch controller, but they also reduce the side-to-side displacements on the tower and the loads on the drive train if a generator torque H_∞ controller is used. Furthermore, in terms of the controller design, instead of using a simple analytical model of a wind turbine, complex linear plants extracted from GH Bladed 4.0 are used, although the design methodology could be applied by using linear models obtained from any modeling package. Regarding the H_∞ controller design, some notch filters are included in the controller dynamics by means of the correct definition of the weight functions in the augmented plant of the mixed sensitivity problem. In the design process of this control strategy based on H_∞ controllers, two software packages are used: GH Bladed 4.0 and MATLAB. GH Bladed is a software package commercialized by Garrad Hassan Company, commonly used by major wind turbine manufacturers to model and simulate wind turbines. The controller synthesis and discretization is carried out in MATLAB and, finally, simulations of the closed loop system are carried out using GH Bladed with different perturbed production winds. Results using H_∞ controllers are compared to the baseline controller results, based on classical control strategies, in order to do a load mitigation analysis to test the load mitigation capacity of the new designed control strategy. In the load analysis, both

In Table 1, the frequencies of these modes are more accurately shown for the operational point of 11 m/s wind speed and some abbreviations are defined as well as referring to the modes used throughout this article. Linear models (1) are expressed by the state-space matrices and have different inputs and outputs. Inputs are the collective pitch angle and generator torque control signals $u(t)$ and the disturbance output $w(t)$ caused by the wind speed. The outputs $y(t)$ are the sensorized measurements used to design the controller. In this case, these outputs are the generator speed w_g , the tower top fore-aft acceleration a_{Tfa} and the tower top side-to-side acceleration a_{Tss} . Due to the non-linear model complexity, and the number of modes taken into account, the order of the linear models is 55. The linear models are not reduced because, after carrying out an analysis, the best quality of the controller syntheses are obtained using high order linear plants and reducing the higher order obtained controllers:

$$\begin{aligned} \dot{X}(t) &= A \cdot X(t) + B_{11} \cdot u(t) + B_{12} \cdot w(t) \\ y(t) &= C \cdot X(t) + D_{11} \cdot u(t) + D_{12} \cdot w(t) \end{aligned} \tag{1}$$

Table 1. Modal analysis of the Upwind model (BW: backward whirl; FW: forward whirl).

Elem.	Mode	Freq. (Hz)	Abbrev.	Elem.	Mode	Freq. (Hz)	Abbrev.
Rotor	In plane 1st	3.68	M_{R1ip}	Rotor	Out of Plane 2nd	2.00	M_{R2op}
	In plane 1st FW	1.31	M_{R1ipfw}		Out of Plane 2st BW	1.80	M_{R2opbw}
	In plane 1st BW	0.89	M_{R1ipbw}	Drive Train	Drive Train	1.66	M_{DT}
	In plane 2st	7.85	M_{R2ip}		1st tower side-to-side	0.28	M_{T1ss}
	In plane 2nd FW	4.30	M_{R2ipfw}	1st tower fore-aft	0.28	M_{T1fa}	
	In plane 2nd BW	3.88	M_{R2ipbw}	2nd tower side-to-side	2.85	M_{T2ss}	
	Out of Plane 1st FW	0.93	M_{R1opfw}	2nd tower fore-aft	3.05	M_{T2fa}	
	Out of Plane 1st	0.73	M_{R1op}	Non-str.	1P	0.2	1P
	Out of Plane 1st BW	0.52	M_{R1opbw}		3P	0.6	3P
	Out of Plane 2nd FW	2.20	M_{R2opfw}				

3. Baseline Classical Control Strategy (C1)

The wind turbine control strategy is defined by a curve (see Figure 2) which relates the generator torque and the generator speed [12]. Three control zones are distinguished in this curve: below rated zone, transition zone and above rated zone. In the below rated zone the control objective is to maintain the power coefficient (C_p) in the optimum value. In the Upwind baseline controller, this is done by means of a generator torque control depending on the generator speed measurement (2). The generator torque T_{br} is proportional to the square of the generator speed by a constant K_{opt} .

$$\begin{aligned} T_{br} &= K_{opt} \cdot w_g^2 \\ K_{opt} &= 2.14 \left[\frac{\text{Nm}}{(\text{rad/s})^2} \right] \end{aligned} \tag{2}$$

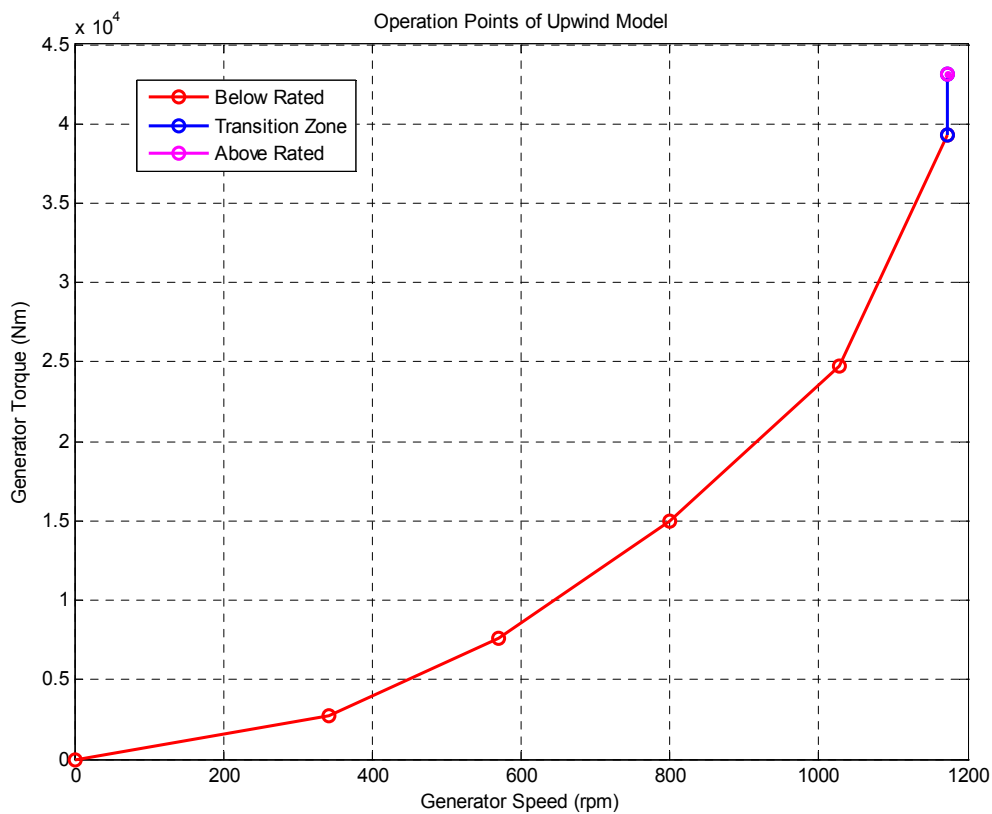
The aim in the transition zone is the control of generator speed by varying the generator torque. In the Upwind model, this can be done with a torque proportional-integral PI (3) controller [13] or with

an open loop torque control which produces a ramp [14] to relate the generator torque and the generator speed. In the C1 control strategy, the *PI* values in the transition zone (wind speed of 11 m/s) used in the Upwind baseline controller are K_{pt} and K_{it} (3), where $u(s)$ is the generator torque control signal and $e(s)$ is the generator speed error:

$$u(s) = \frac{K_{pt}s + K_{it}}{s} \cdot e(s)$$

$$K_{pt} = 4200 ; K_{it} = 2100 \tag{3}$$

Figure 2. Curve of power production control zones for the Upwind wind turbine.



In the above rated zone, the goal is the generator speed control at the nominal value of 1173 rpm varying the collective pitch angle in the blades to maintain the electric power at the value of 5 MW. To do this, a gain-scheduled (*GS*) *PI* controller [15] is used. In this case, the controller input $u(s)$ is the generator speed error, and the controller output $\beta_{col}(s)$ is the collective pitch angle control signal. The linear plants used to tune the gain-scheduled *PI* controller are the plants which relate pitch angle and generator speed. These plants have different gains, so gain-scheduling is used to guarantee the stability of the closed loop system in spite of the gain differences. To develop the gain-scheduling, two *PI* controllers (4) in two operational points, winds of 13 m/s and 21 m/s, are tuned:

$$K_{pt_{13}} = 0.009; K_{it_{13}} = 0.003$$

$$K_{pt_{21}} = 0.0039; K_{it_{21}} = 0.0013 \tag{4}$$

In the other operational points, the *PI* parameters are extrapolated by a first order approximation. A similar gain-scheduling strategy is proposed in [14]. Instead of using the wind speed signal from the

anemometer, this PI is scheduled by the collective pitch angle in the blades. The corresponding steady-state collective pitch angle is 6.42° for the operational point with a wind speed of 13 m/s, and the corresponding steady-state collective pitch angle value is 18.53° for the operational point with a wind speed of 21 m/s. Finally, some series notch filters are useful to improve the PI controller response [16]. Some design criteria are established to tune these controllers in these operational points:

1. Output sensitivity peak: 6 dB approximately.
2. Open loop phase margin between 30 and 60 degrees.
3. Open loop gain margin between 6 and 12 dB.
4. To maintain constant the PI zero frequency.

The drive train damping filter (DTD) is included. The aim of the DTD is to reduce the wind effect on the drive train mode [15,17]. The DTD for the Upwind model (5) consists of one gain, with one differentiator, one real zero and a pair of complex poles:

$$T_{DTD}(s) = \left[K_1 \cdot \frac{s \left(1 + \frac{1}{w_1} s \right)}{\left(\left(\frac{1}{w_2} \right)^2 s^2 + 2\xi_2 \frac{1}{w_2} s + 1 \right)} \right] \cdot w_g(s) \quad (5)$$

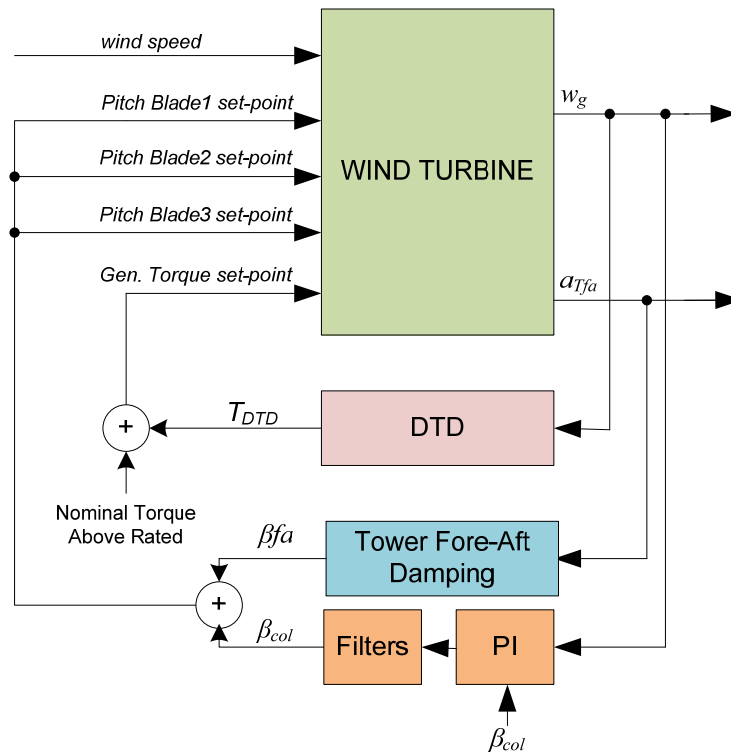
$$K_1 = 641.45 \text{ Nms/rad}; \quad w_1 = 193 \text{ rad/s}; \quad w_2 = 10.4 \text{ rad/s}; \quad \xi_2 = 0.984$$

The input of the filter is the generator speed w_g and the output is a contribution T_{DTD} to the generator torque set-point signal. Finally, the tower fore-aft damping filter (TD) is designed to reduce the wind effect on the tower first fore-aft mode in the above rated power production zone [15,17]. For the Upwind baseline controller, the filter (6) consists of a gain with one integrator, a pair of complex poles and a pair of complex zeros:

$$B_{fa}(s) = K_{TD} \cdot \frac{1}{s} \cdot \left[\frac{1 + (2 \cdot \zeta_{T1} \cdot s / w_{T1}) + (s^2 / w_{T1}^2)}{1 + (2 \cdot \zeta_{T2} \cdot s / w_{T2}) + (s^2 / w_{T2}^2)} \right] \cdot a_{Tfa}(s) \quad (6)$$

$$K_{TD} = 0.035; \quad w_{T1} = 1.25 \text{ rad/s}; \quad \zeta_{T1} = 0.69; \quad w_{T2} = 3.14 \text{ rad/s}; \quad \zeta_{T2} = 1$$

The input of the filter is the fore-aft acceleration measured in the tower top a_{Tfa} and the output is a pitch contribution β_{fa} to the collective pitch angle. In conclusion, the baseline control strategy is defined in Figure 3. Other strategies to reduce the loads on the wind turbine can be developed, but they are not included in the considered baseline controller.

Figure 3. Baseline C1 control strategy.

4. Objectives for Designing the New Proposed Control Strategy

The control objectives for the developed wind turbine control strategy working in the above rated power production zone are as follows:

1. Generator speed control (increase of the output sensitivity bandwidth and reduction of the peak in comparison with the baseline controller).
2. To mitigate the load on the drive train reducing the wind effect on the drive train mode.
3. To mitigate the load on the tower reducing the wind effect on the tower first modes (side-to-side and fore-aft).
4. To improve the load mitigation in comparison to a baseline controller based on the classical baseline control strategy.

To achieve these control objectives, a generator speed sensor and an accelerometer on the tower top are used [18].

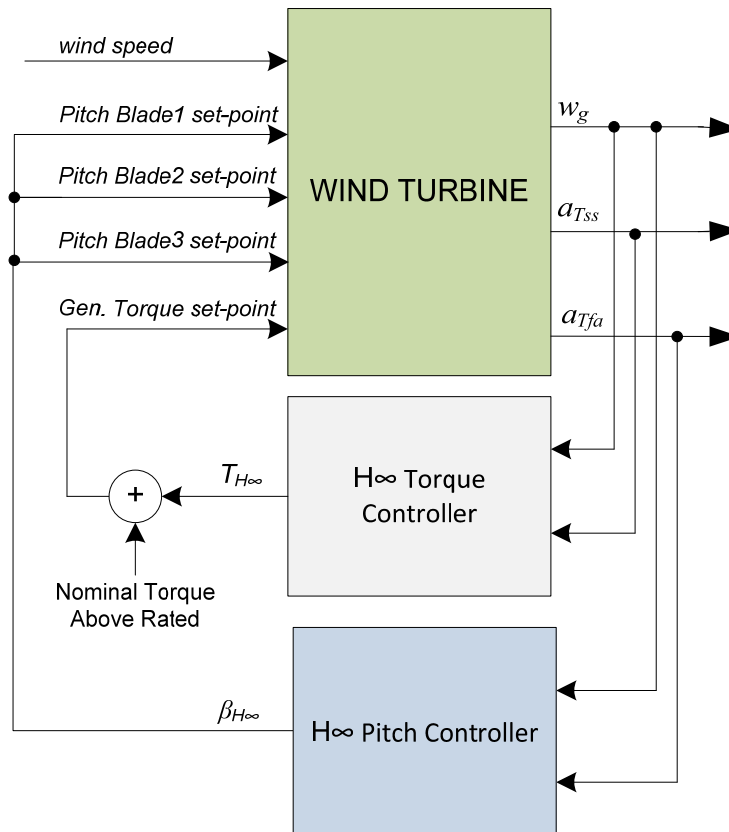
5. New Proposed Control Strategy Based on H_∞ Norm Reduction (C2)

5.1. Design of Control Strategy Based on H_∞ Norm Reduction

This strategy consists of two robust, multivariable and multi-objective controllers based on the H_∞ norm reduction (see Figure 4). The generator torque controller and the pitch controller are designed separately [19]. The torque controller has two inputs (generator speed w_g and tower top side-to-side acceleration a_{Tss}) and one output (generator torque control signal $T_{H\infty}$). On the other hand, the pitch controller has two inputs (generator speed w_g and tower top fore-aft acceleration a_{Tfa}) and one output

(collective pitch control signal β_{H_∞}). The collective pitch angle set-point value is the pitch control signal β_{H_∞} . However, the generator torque set-point value is the addition of the generator torque control signal T_{H_∞} and the generator torque nominal value in the above rated zone.

Figure 4. C2 control strategy based on the H_∞ norm reduction.



The control design method can be divided into the following steps:

1. To extract the wind turbine linear models from the GH Bladed non-linear model. The wind turbine used for this design is the 5 MW Upwind model.
2. To analyze the linear models in Simulink extracting the Campbell Diagram.
3. To design the torque H_∞ controller in MATLAB.
4. To design the pitch H_∞ controller in MATLAB taking into account the previous designed H_∞ torque controller.
5. To analyze the controller robustness in MATLAB.
6. To test the controllers in Simulink.
7. To include the controllers in the GH Bladed External Controller.
8. To simulate the GH Bladed non-linear model using the designed two MISO H_∞ controllers.
9. To compare the time domain and frequency domain results to the baseline classical controller.
10. To analyze the fatigue loads and extreme loads reduction of the proposed control strategy compared to the baseline control strategy.

5.2. Generator Torque Controller (H_∞ Torque Controller)

The designed generator torque controller based on the H_∞ norm reduction solves two of the control objectives proposed in Section 4:

1. To reduce the wind effect on the drive train mode M_{DT} .
2. To reduce the wind effect on the tower side-to-side mode M_{T1ss} .

To design the controller, a mixed sensitivity problem (7) will be solved. The nominal plant $G(s)$ is selected at the operational point of 19 m/s wind speed and has one input T (generator torque), two outputs w_g and a_{Tss} and 55 states (see Figure 5). $G_{11}(s)$ is the plant with a generator torque input and a generator speed output, while $G_{12}(s)$ is the plant with a generator torque input and a tower top side-to-side acceleration output. p_1 and p_2 are the disturbance outputs of the plant, u is the control signal, y_1 and y_2 are the controller inputs, and Zp_{11} , Zp_{12} , Zp_2 , Zp_{31} and Zp_{32} are the performance outputs. The augmented plant (see Figure 6) of this mixed sensitivity problem is scaled using the constants Du , De_1 , De_2 , Dp_1 and Dp_2 (8).

Figure 5. Family of plants for the H_∞ torque controller design.

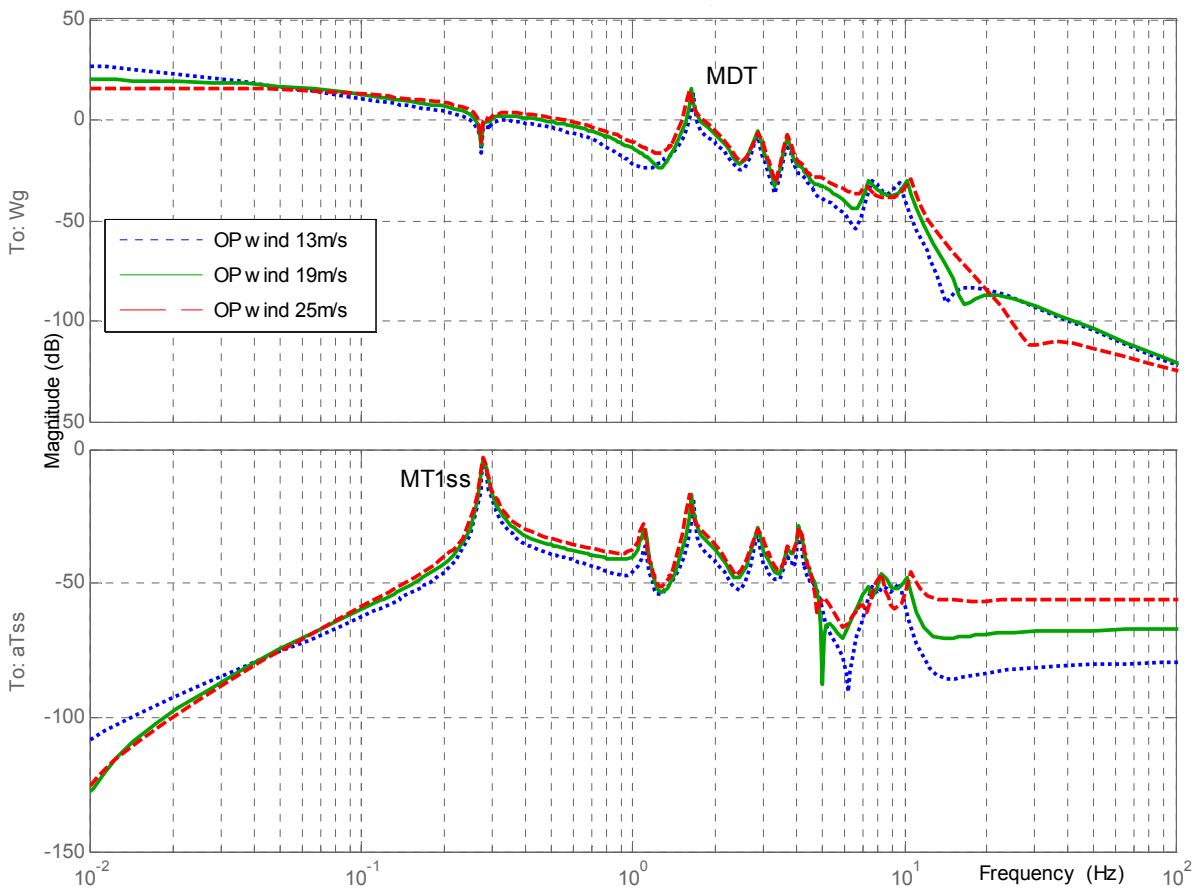
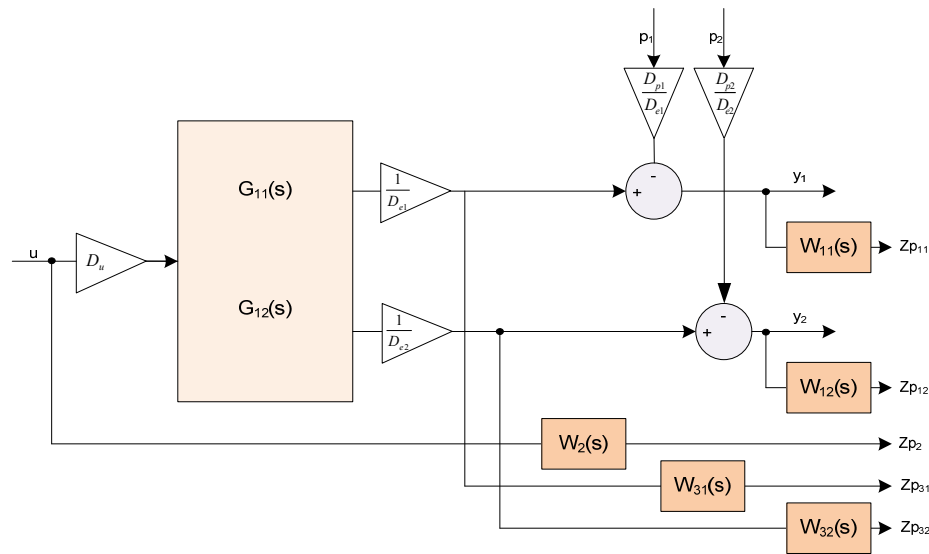


Figure 6. Augmented plant for the MISO Mixed-Sensitivity Problem.



$$\begin{pmatrix} Zp_{11} \\ Zp_{12} \\ Zp_2 \\ Zp_{31} \\ Zp_{32} \\ y_1 \\ y_2 \end{pmatrix} = \begin{pmatrix} -\frac{Dp_1}{De_1} \cdot W_{11} & 0 & \frac{Du}{De_1} \cdot G_{11}(s) \cdot W_{11} \\ 0 & -\frac{Dp_2}{De_2} \cdot W_{12} & \frac{Du}{De_2} \cdot G_{12}(s) \cdot W_{12} \\ 0 & 0 & W_2 \\ 0 & 0 & \frac{Du}{De_2} \cdot G_{11}(s) \cdot W_{31} \\ 0 & 0 & \frac{Du}{De_1} \cdot G_{12}(s) \cdot W_{32} \\ -\frac{Dp_1}{De_1} & 0 & \frac{Du}{De_1} \cdot G_{11}(s) \\ 0 & -\frac{Dp_2}{De_2} & \frac{Du}{De_2} \cdot G_{12}(s) \end{pmatrix} \cdot \begin{pmatrix} p_1 \\ p_2 \\ u \end{pmatrix} \tag{7}$$

The uncertainties of the family of plants are not considered in this mixed sensitivity problem due to the fact that the drive train and tower modes frequencies do not considerably vary in the above rated zone. The weight functions (9) W_{31} and W_{32} are not used, so their values are 1 in order not to consider them in the MATLAB Robust Toolbox [20]. W_{11} is an inverted notch filter centred on the M_{DT} frequency and W_{12} is another inverted notch filter centred on the M_{T1ss} frequency. W_2 is an inverted low-pass filter used to reduce the controller activity in high frequencies (see Figure 7):

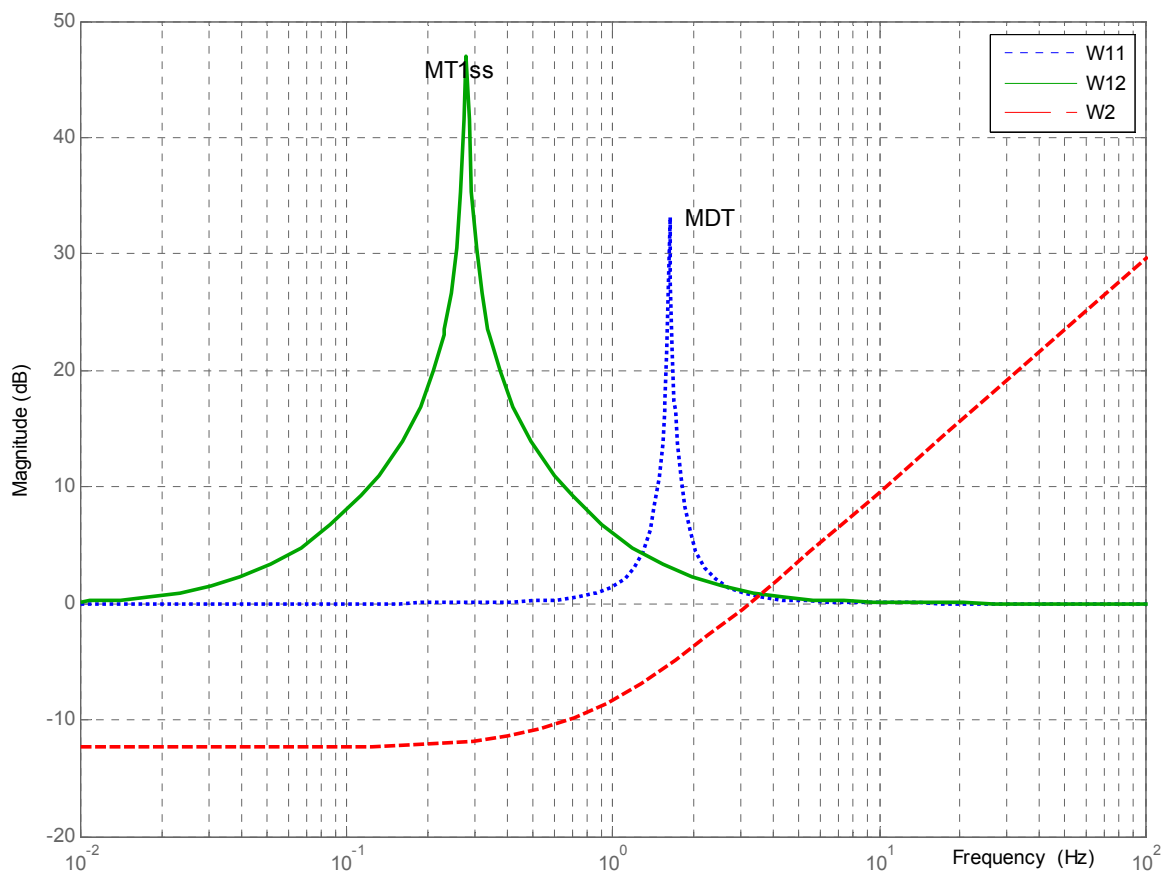
$$Du = 90; De_1 = 0.1; De_2 = 1; Dp_1 = 0.1; Dp_2 = 1 \tag{8}$$

$$W_{11}(s) = \frac{(s^2 + 6.435s + 104.9)}{(s^2 + 0.1416s + 104.9)}$$

$$W_{12}(s) = \frac{(s^2 + 9.984s + 3.117)}{(s^2 + 0.04437s + 3.117)} \tag{9}$$

$$W_2(s) = \frac{30000(s + 5.027)}{(s + 6.823e5)}$$

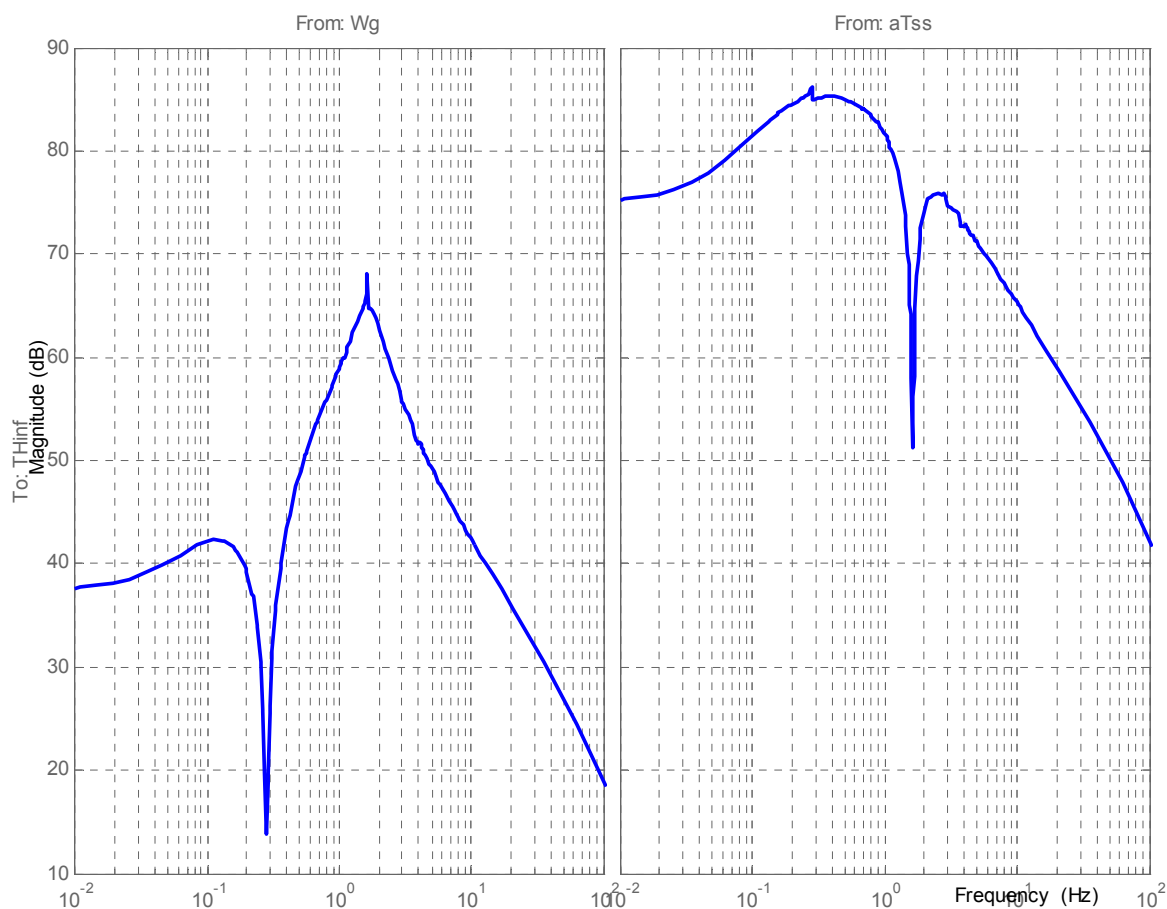
Figure 7. Weight functions for H_∞ torque controller design.



After doing the controller synthesis, the obtained controller (see Figure 8) has to be re-scaled to adapt the inputs and the outputs to the real non-scaled plant. The obtained controller order is 39 but, finally, the controller order is reduced to order 25 and discretized using a sample time of 0.01 s. The discretized controller is represented by the state space matrices A_{TD} , B_{TD} , C_{TD} and D_{TD} (10):

$$\begin{aligned}
 X_{TD}(k+1) &= A_{TD} \cdot X_{TD}(k) + B_{TD} \cdot \begin{pmatrix} e_{wg}(k) \\ a_{Tss}(k) \end{pmatrix} \\
 T_{H_\infty}(k) &= C_{TD} \cdot X_{TD}(k) + D_{TD} \cdot \begin{pmatrix} e_{wg}(k) \\ a_{Tss}(k) \end{pmatrix}
 \end{aligned}
 \tag{10}$$

Figure 8. H_∞ Torque Controller.



5.3. Collective Pitch Angle Controller (H_∞ Pitch Controller)

The collective pitch H_∞ MISO controller solves the other control objectives:

1. Generator speed control increasing the closed loop disturbance attenuation bandwidth.
2. Reduction of the wind effect on the tower fore-aft mode.
3. Inclusion of notch filters at particular frequencies in the controller dynamics to mitigate other excited frequencies (see Table 2) in the nominal plant.

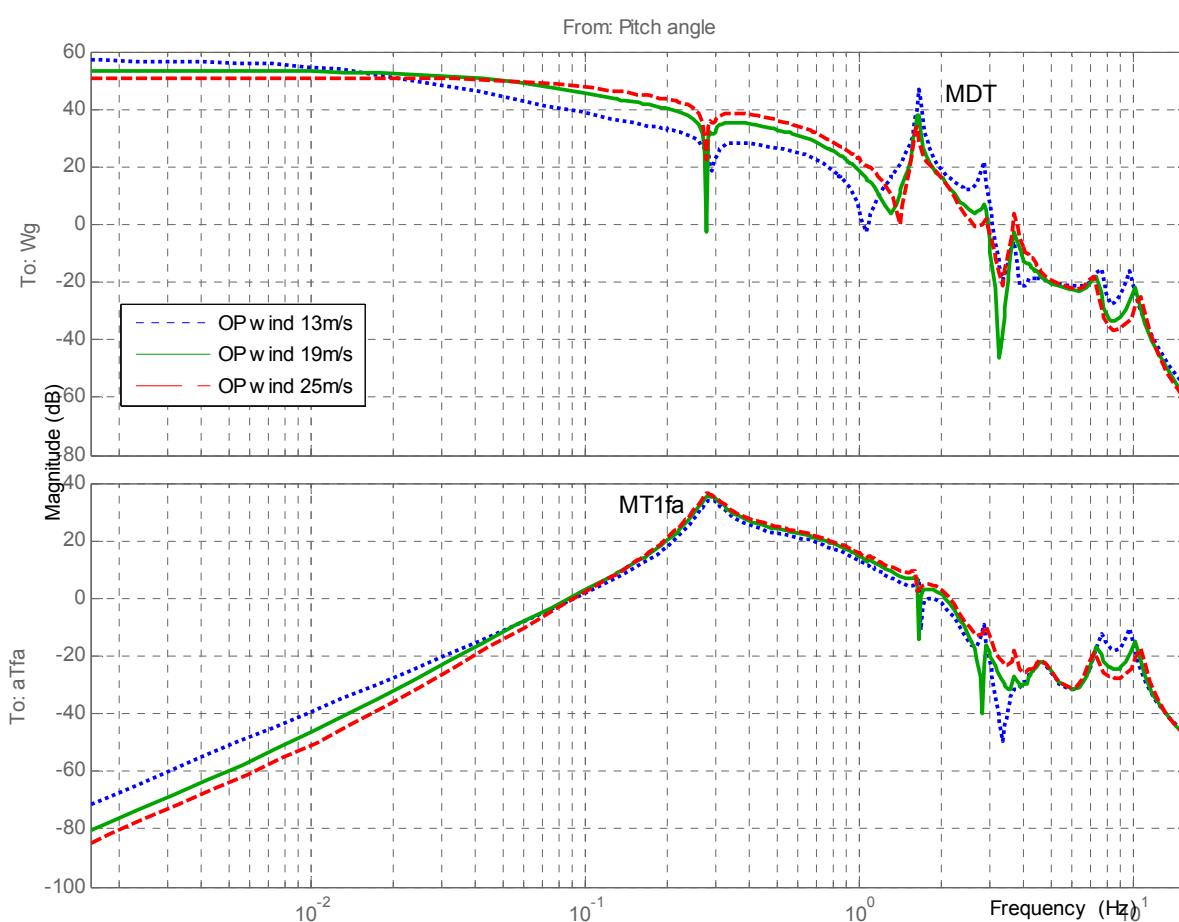
Table 2. Frequency of notch filters in the H_∞ Pitch Controller.

Mode	Freq. (Hz)
1P	0.20
3P	0.60
M_{T2ss}	2.86
M_{R1ip}	3.69
M_{R2ip}	7.36

Another mixed sensitivity problem is proposed to develop this controller. In this case, the nominal plant $GI(s)$ is selected for the operational point of 19 m/s wind speed (see Figure 9), it has one input β (collective pitch angle), two outputs w_g and a_{Tfa} and considers the coupling caused by the inclusion of the H_∞ MISO torque controller designed in the previous section. $G_{11}(s)$ is the plant with a collective pitch input and a generator speed output and $G_{12}(s)$ is the plant with a collective pitch input and the tower top fore-aft acceleration output. This control scenario has new scaled constants (11) and the family of plants is considered as an additive uncertainty model due to the variations of the linear plants according to the operational point in the above rated zone:

$$Du = 1; De_1 = 10; De_2 = 0.1; Dp_1 = 10; Dp_2 = 0.1 \tag{11}$$

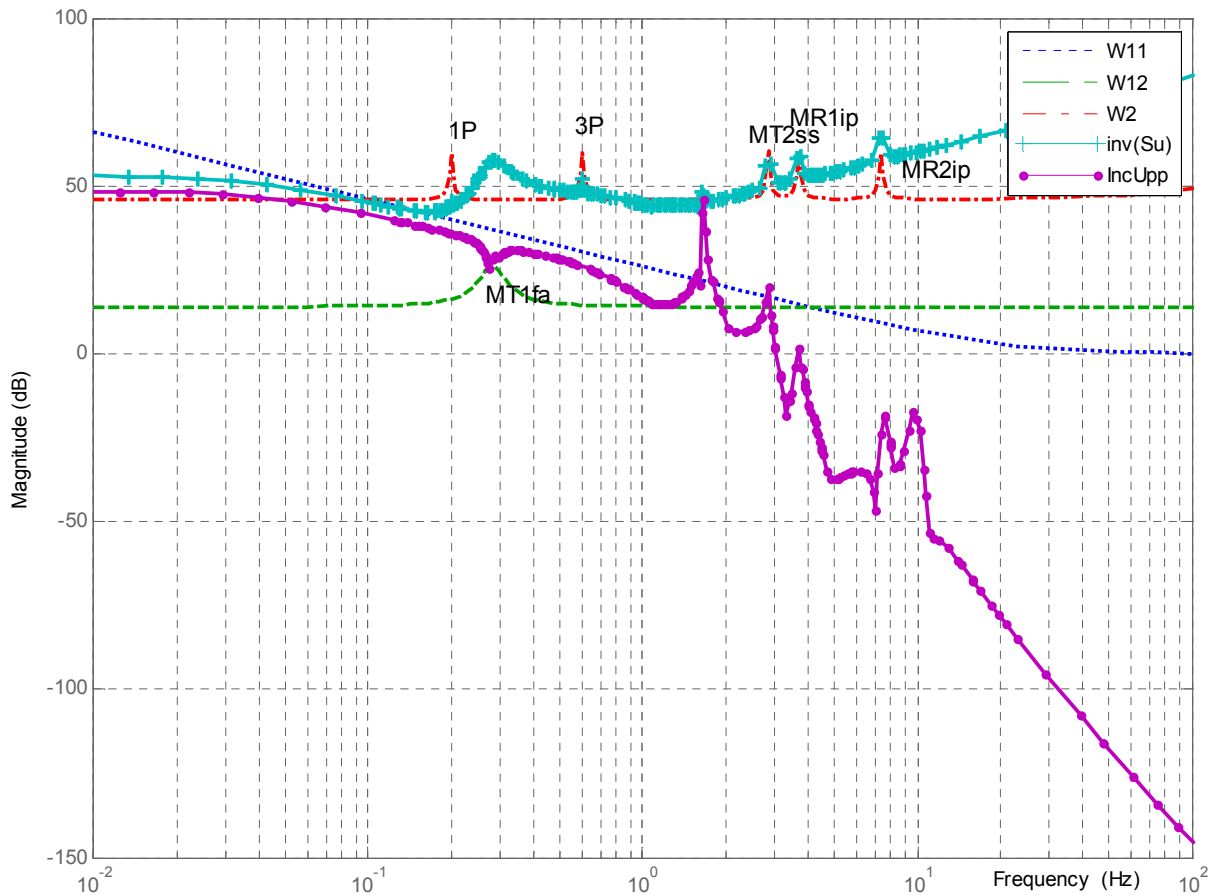
Figure 9. Family of plants for the H_∞ pitch controller design.



Regarding the weight functions (12) in this mixed sensitivity problem, the W_{11} is an inverted high-pass filter which determines the desired profile of the output sensitivity function. W_{12} is an inverted notch filter centred on the M_{T1fa} and W_2 is an inverted low-pass filter used to reduce the controller activity in high frequencies, including some inverted notch filters centred on excited frequencies (see Table 2) to include notch filters in the pitch controller dynamics (see Figure 10).

$$\begin{aligned}
 W_{11}(s) &= \frac{(s + 125.7)}{(s + 6.283e-5)} \\
 W_{12}(s) &= \frac{(5s^4 + 5.733s^3 + 31.58s^2 + 18s + 49.28)}{(s^4 + 0.3117s^3 + 6.288s^2 + 0.9786s + 9.856)} \\
 W_2(s) &= \frac{200000(s + 628.3)(s^2 + 0.1005s + 1.579)(s^2 + 0.3016s + 14.21)}{(s + 6.283e5)(s^2 + 0.02011s + 1.579)(s^2 + 0.06032s + 14.21)} \\
 &\quad \cdot \frac{(s^2 + 1.438s + 322.9)(s^2 + 1.885s + 537.5)(s^2 + 3.7s + 2139)}{(s^2 + 0.2875s + 322.9)(s^2 + 0.371s + 537.5)(s^2 + 0.7399s + 2139)}
 \end{aligned}
 \tag{12}$$

Figure 10. Weight functions for the H_∞ pitch controller design.



The gains of the upper uncertainty model IncUpp are bounded by W_2 weight functions (see Figure 8) to guarantee the robust controller design. After re-scaling the obtained controller (see Figure 11), whose order is 45, it is reduced to order of 24 and discretized using a sample time of 0.01 s. The discretized controller is represented by the state space matrices A_{BD} , B_{BD} , C_{BD} and D_{BD} (13):

$$\begin{aligned}
 X_{BD}(k + 1) &= A_{BD} \cdot X_{BD}(k) + B_{BD} \cdot \begin{pmatrix} e_{wg}(k) \\ a_{Tfa}(k) \end{pmatrix} \\
 \beta_{H\infty}(k) &= C_{BD} \cdot X_{BD}(k) + D_{BD} \cdot \begin{pmatrix} e_{wg}(k) \\ a_{Tfa}(k) \end{pmatrix}
 \end{aligned}
 \tag{13}$$

Figure 11. H_∞ Pitch Controller.

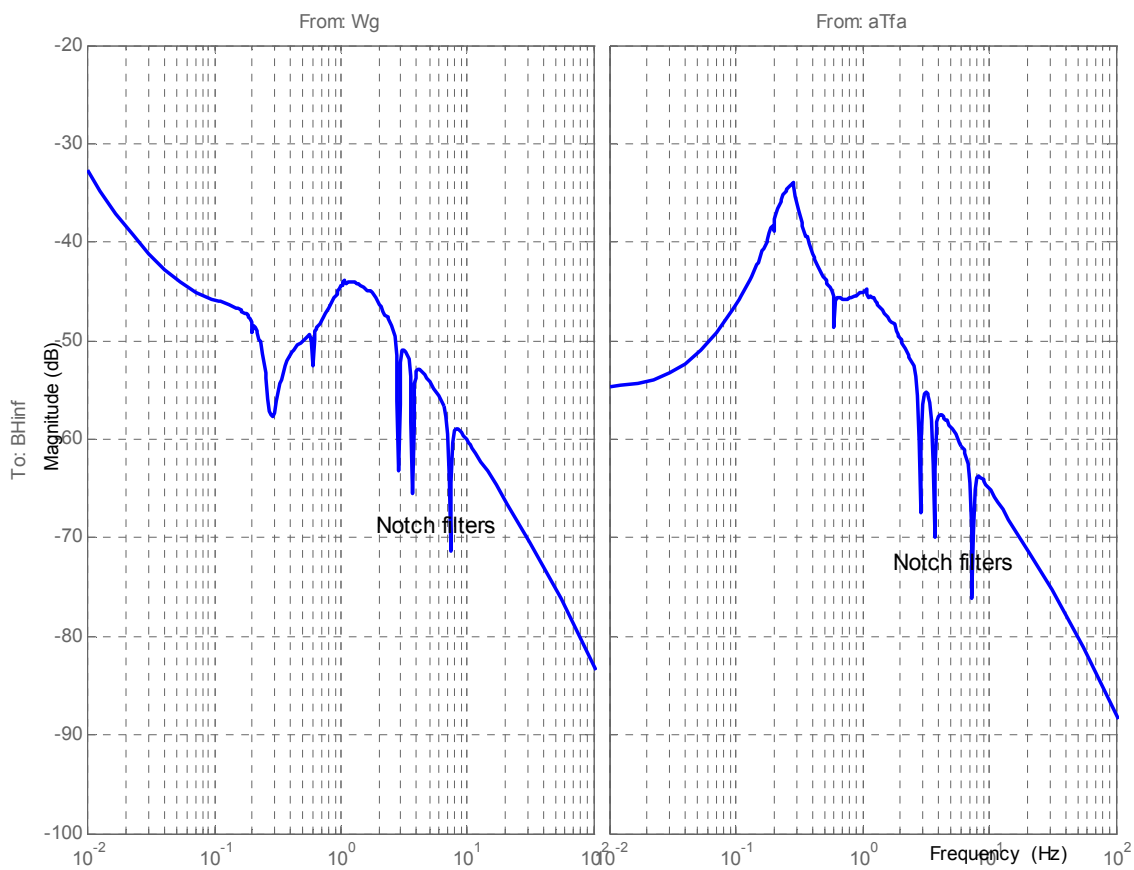
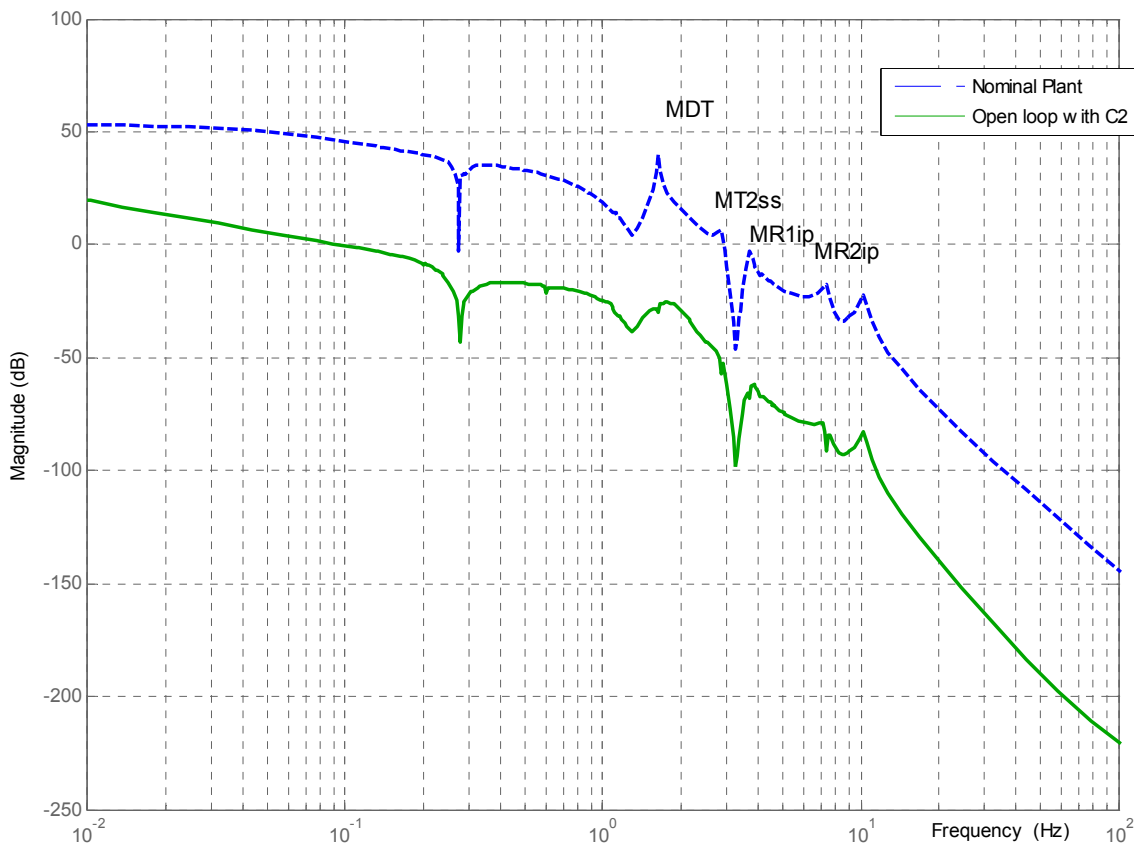


Figure 12. Effect of the pitch controller notch filter in open loop.



5.4. Analysis of the H_∞ Control Strategy

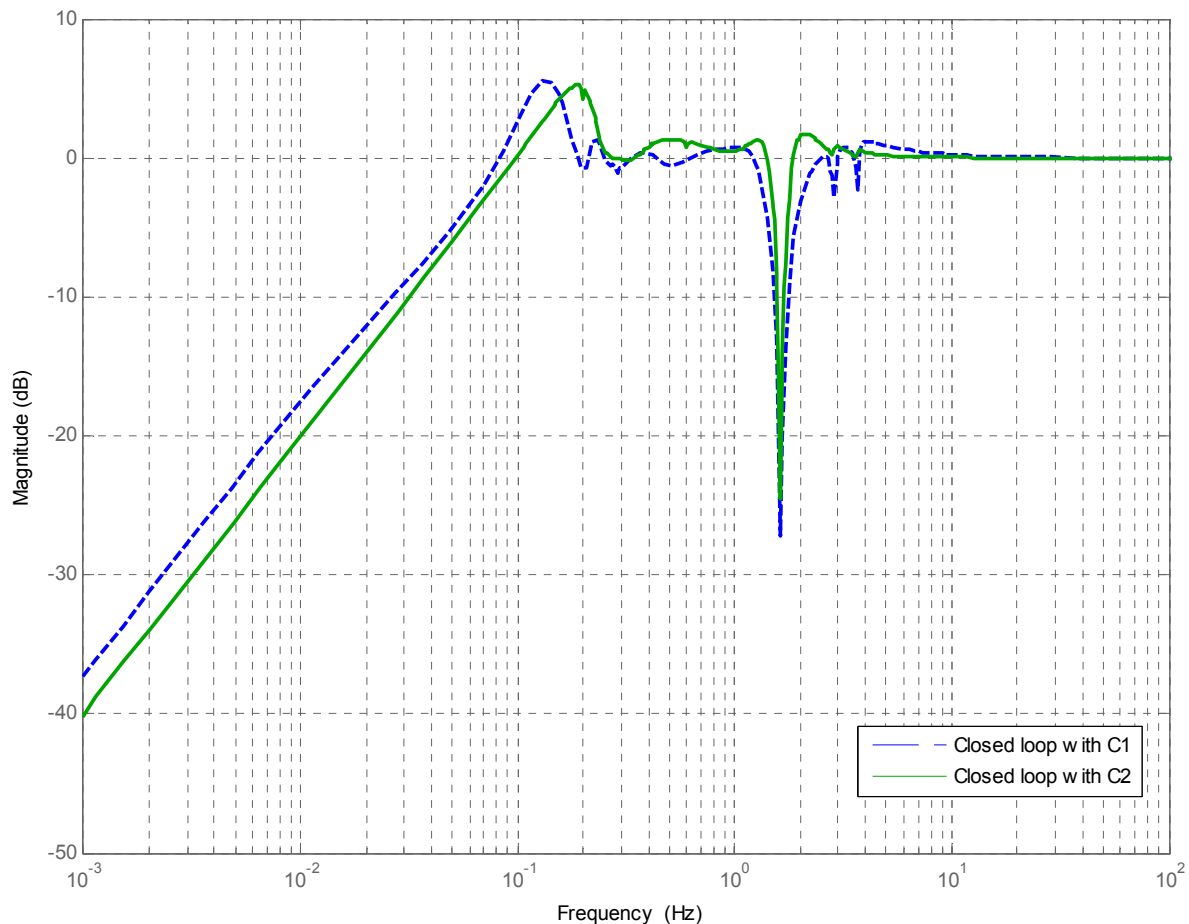
Gain variations in the generator speed control are only considered in the controller robust analysis due to the fact that the tower and drive train modes for the Upwind model have constant frequencies in the above rated zone. The controller robustness is guaranteed because the gains of the upper uncertainty model IncUpp are bounded by the inverse of the control sensitivity function S_u [21] (see Figure 10). To compare the response of the designed controllers to the baseline controller, the two control strategies in the above rated zone are considered:

- **C1:** Baseline control strategy with drive train damping filter and tower fore-aft damping filter activated (see Figure 3).
- **C2:** Proposed control strategy with two H_∞ MISO controllers.

Using the C2 control strategy, the generator speed output disturbance attenuation bandwidth DABW in the different operational points is higher than using the baseline control strategy (see Table 3) and the generator speed output disturbance attenuation peak DAP is lower near the designed wind speed nominal operational point of 19 m/s. For the nominal plant, for which the controller is designed, the generator speed output sensitivity function (see Figure 13) shows the peak and the bandwidth to control the generator speed output for a generator speed output disturbance. This sensitivity function clearly shows the increase in the bandwidth achieved with the H_∞ C2 control strategy. These improvements are of interest in order to reduce extreme loads, as will be shown in section 6. The reduction of the wind effect on the M_{DT} drive train mode is critical for the control strategy design, so it has been designed first. This mode reduction appears in the wind effect on different parts of the wind turbine due to the hard coupling of this mode in the system. For example, Figure 12 shows the M_{DT} mitigation in the plant which relates the generator speed frequency response for a pitch angle input. Figure 14 shows the frequency response of the tower side-side acceleration for a wind input where the drive train mode is mitigated clearly with the C1 and C2 control strategies compared to the plant without the control system.

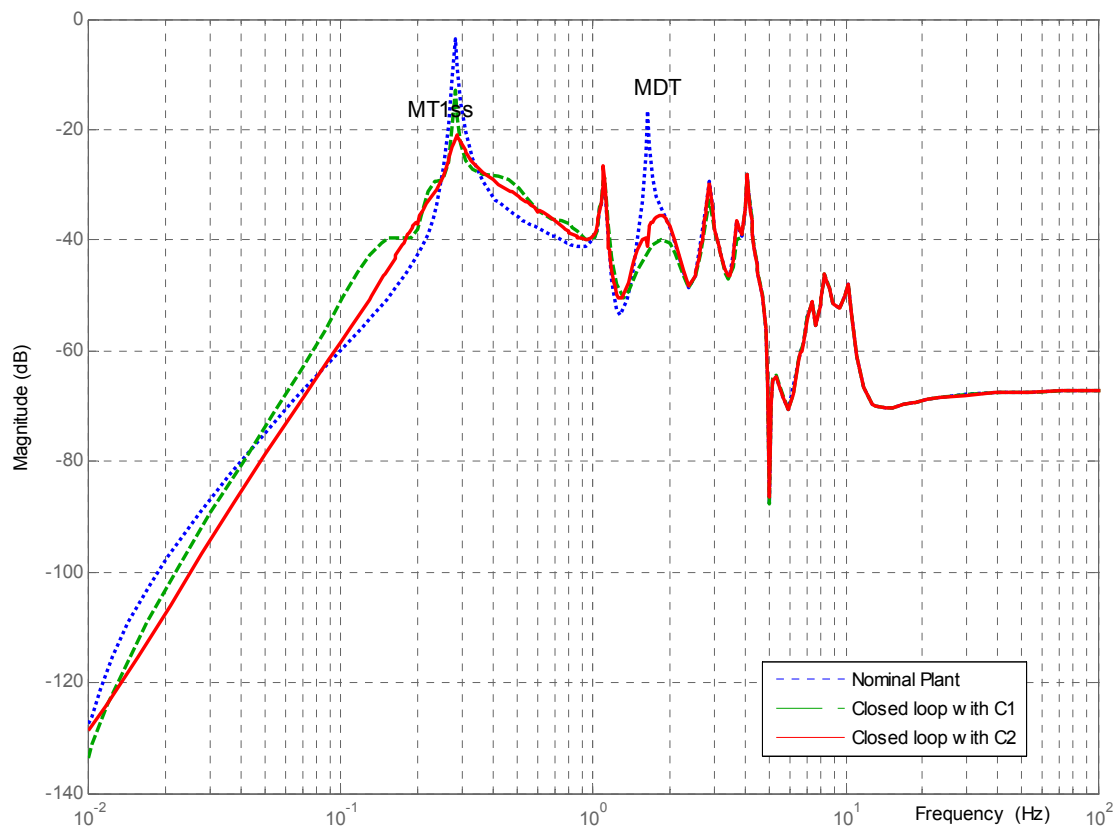
Table 3. Comparison of generator speed disturbance attenuation.

OP (m/s)	C1		C2	
	DABW (Hz)	DAP (dB)	DABW (Hz)	DAP (dB)
13	0.037	6.06	0.035	3.35
15	0.045	6.06	0.044	3.59
17	0.052	6.09	0.057	4.31
19	0.058	6.31	0.070	5.29
21	0.061	6.00	0.078	5.78
23	0.065	6.05	0.089	6.70
25	0.069	6.04	0.10	7.84

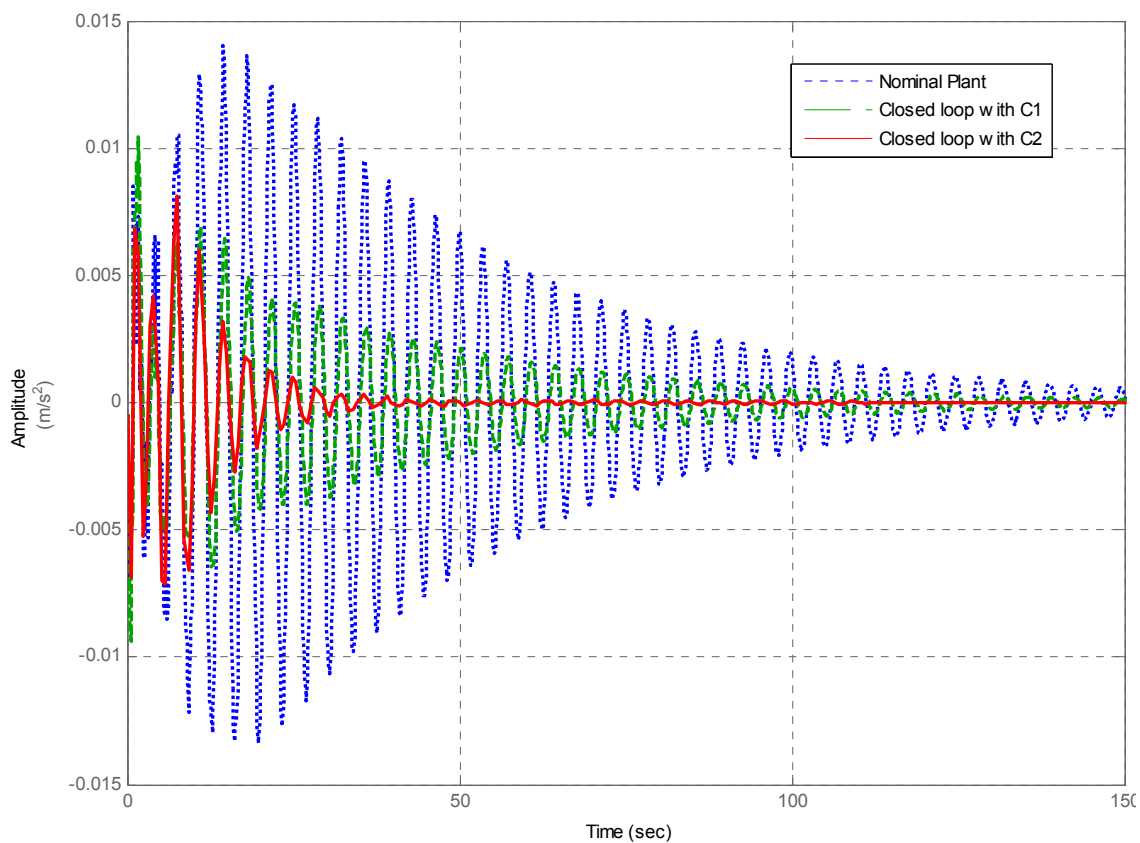
Figure 13. Generator speed output sensitivity function.

To analyze the reduction of the fore-aft and side-to-side tower accelerations due to the mitigation of the wind effect on these modes using the H_∞ control strategy, the closed loop response has to be analyzed in time and frequency domains for the two control strategies. The frequency response of the tower top side-to-side acceleration for a wind input (see Figure 14) is mitigated at the M_{T1ss} frequency using the C2 control strategy, but this mode is not reduced when the C1 strategy is used because it was not designed for that. This gain reduction at this frequency involves an amplitude reduction of the tower side-to-side acceleration in time domain (see Figure 14). The frequency response of the tower top fore-aft acceleration for a wind input (see Figure 15) is mitigated at the M_{T1fa} frequency using the C1 and C2 control strategies. This mode is not very excited in the Upwind model, but this mitigation could be more useful in other wind turbine models. This gain reduction at the peak of the M_{T1fa} mode involves an amplitude reduction of the tower fore-aft acceleration in time domain. The gain mitigation on the M_{T1fa} and M_{T1ss} frequencies is important to reduce the momentums in the tower y and x axis respectively, and the momentum reductions mean load mitigations on the tower.

Figure 14. Tower top side-to-side acceleration response for a wind input (a) Frequency response; (b) Time domain wind step response.

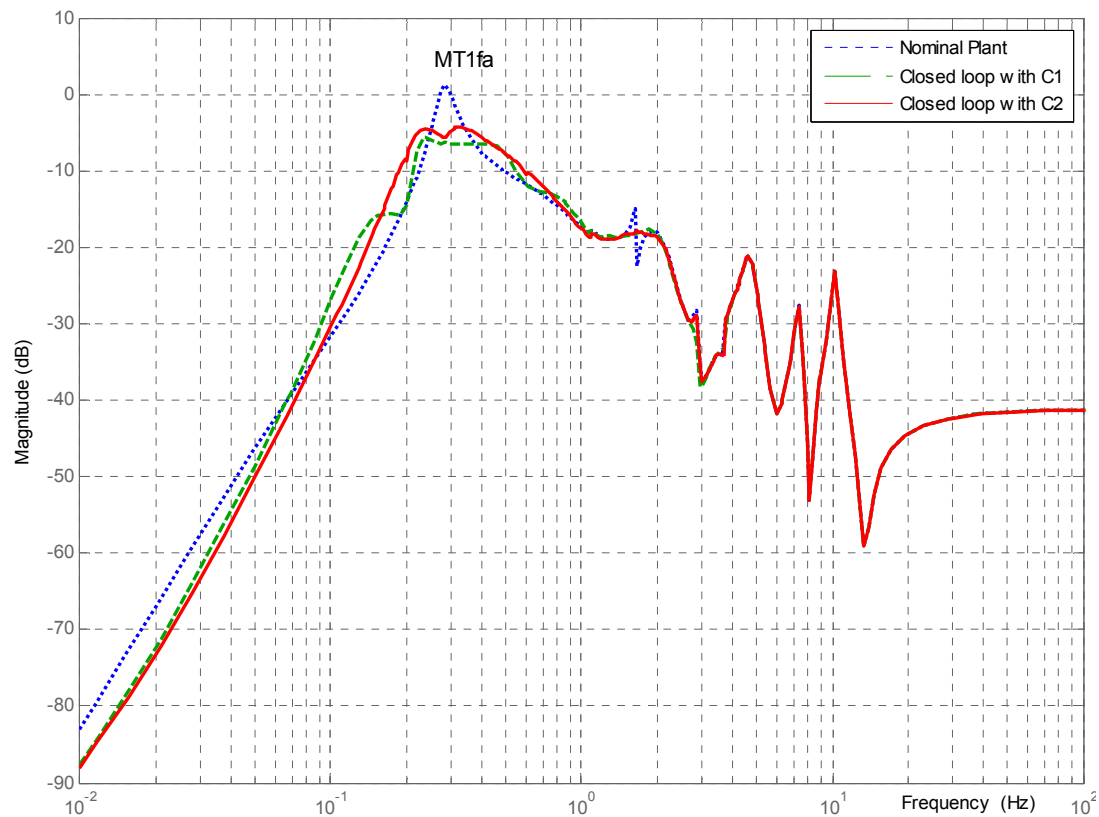


(a)

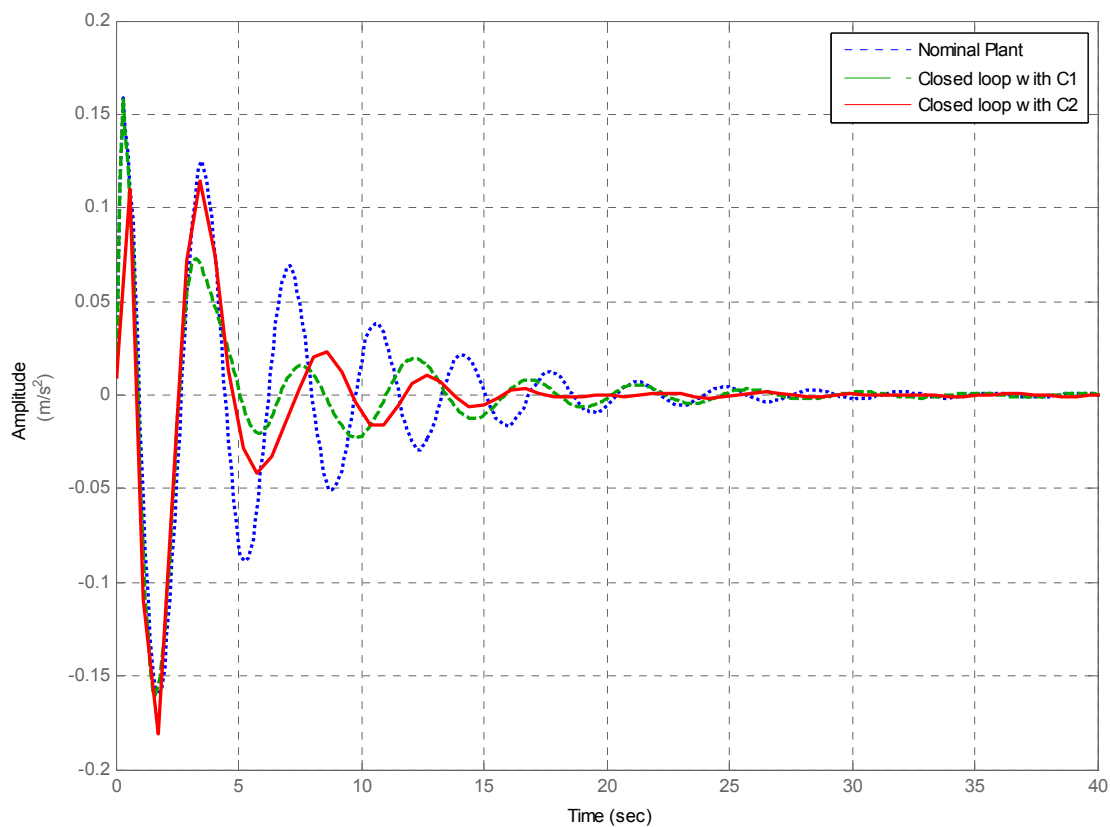


(b)

Figure 15. Tower top fore-aft acceleration response for a wind input (a) Frequency response; (b) Time domain wind step response.



(a)



(b)

Finally, the notch filters included in the pitch controller dynamics are used to mitigate other excited frequencies which appear in the plant which relates the pitch angle with the generator speed. In this plant (see Figure 12), for the operational point of wind 19 m/s, the structural modes M_{T2ss} , M_{R1ip} , M_{R2ip} are excited and they are mitigated using the H_∞ C2 control strategy. The effect of the notch filters at the frequencies $1P$ and $3P$ (blade passing frequencies) are only observed in the frequency analysis of the time domain simulations, because the excitations in these frequencies are not expressed in the linear plants extracted from GH Bladed.

6. Results in GH Bladed

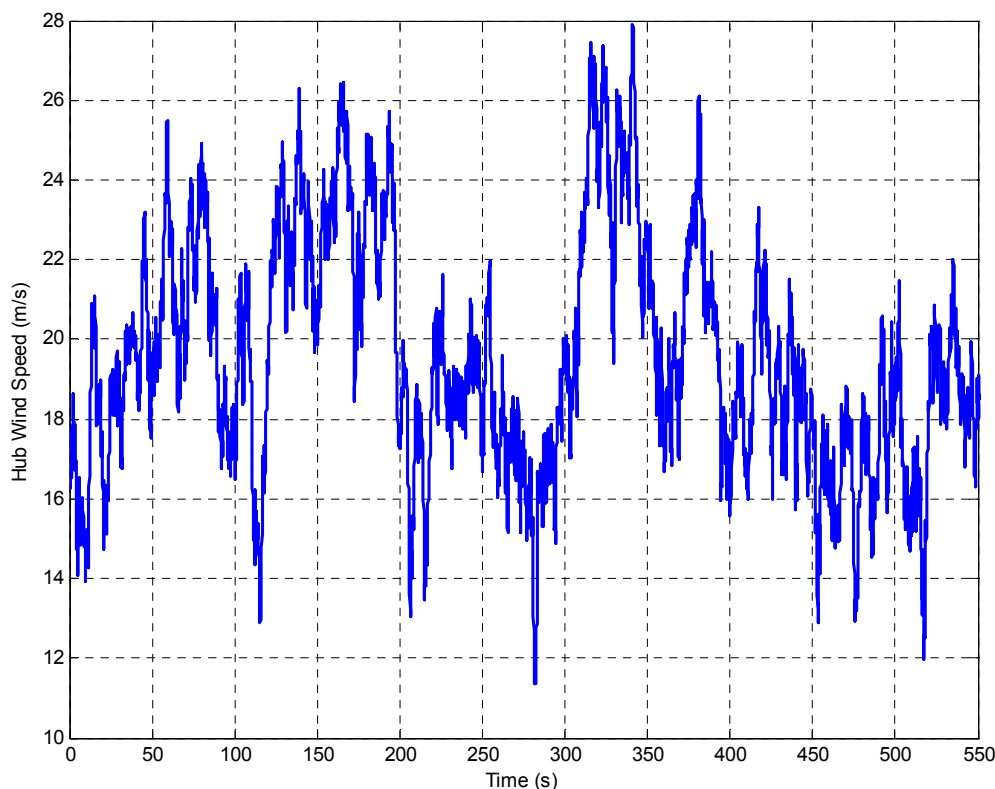
6.1. External Controller in GH Bladed

The two H_∞ MISO controllers are included in the External Controller in GH Bladed to do time domain simulations using the Upwind wind turbine non-linear model. The External Controller [22] is the name of the programmed code to control the wind turbine non-linear model in GH Bladed. GH Bladed calls to the External dynamic library .dll with the frequency determined by the sample time of the control strategy. The C1 and C2 control strategies are included in the External Controller to carry out the control strategies in the above rated power production zone. However, the control strategy in the below rated and transition zones is the same as the baseline control strategy and it is described in section 3. For a more realistic comparison between the results using the C1 control strategy and the results using the C2 control strategy in the above rated zone, the C2 strategy is divided into two cases:

- **C2.1:** The accelerometer to measure the tower top side-to-side acceleration is disabled. This is done to compare C1 and C2 control strategies without tower side-to-side damping.
- **C2.2:** The tower top side-to-side accelerometer is activated and C2 control strategy works without sensor signals restrictions (see Figure 4).

In the control strategy based on the H_∞ MISO discretized controllers, the control signals are calculated for each sample time (0.01 s) using the present vector of states expressed in the state-representation of the controller dynamics. The sample time has been selected after consulting wind turbine manufacturer references. The strategy to calculate the controller output is divided into four steps:

1. To initialize the controller state-space matrices A , B , C , and D from a static library and initialize the actual state vector $X(k)$.
2. To update the present vector of controller inputs $e(k)$ reading the wind turbine measurements from the sensors.
3. To calculate the vector of present controller outputs $u(k)$ using matrices C , D and the current vectors of controller inputs $e(k)$ and states $X(k)$.
4. To calculate the vector of the next sample time controller states $X(k)$ using matrices A and B and the actual vectors of controller inputs $e(k)$ and states $X(k)$. In the next sample time this vector of controller states will be the current vector of controller states.

Figure 16. Hub wind speed for a turbulent production wind of 19 m/s.

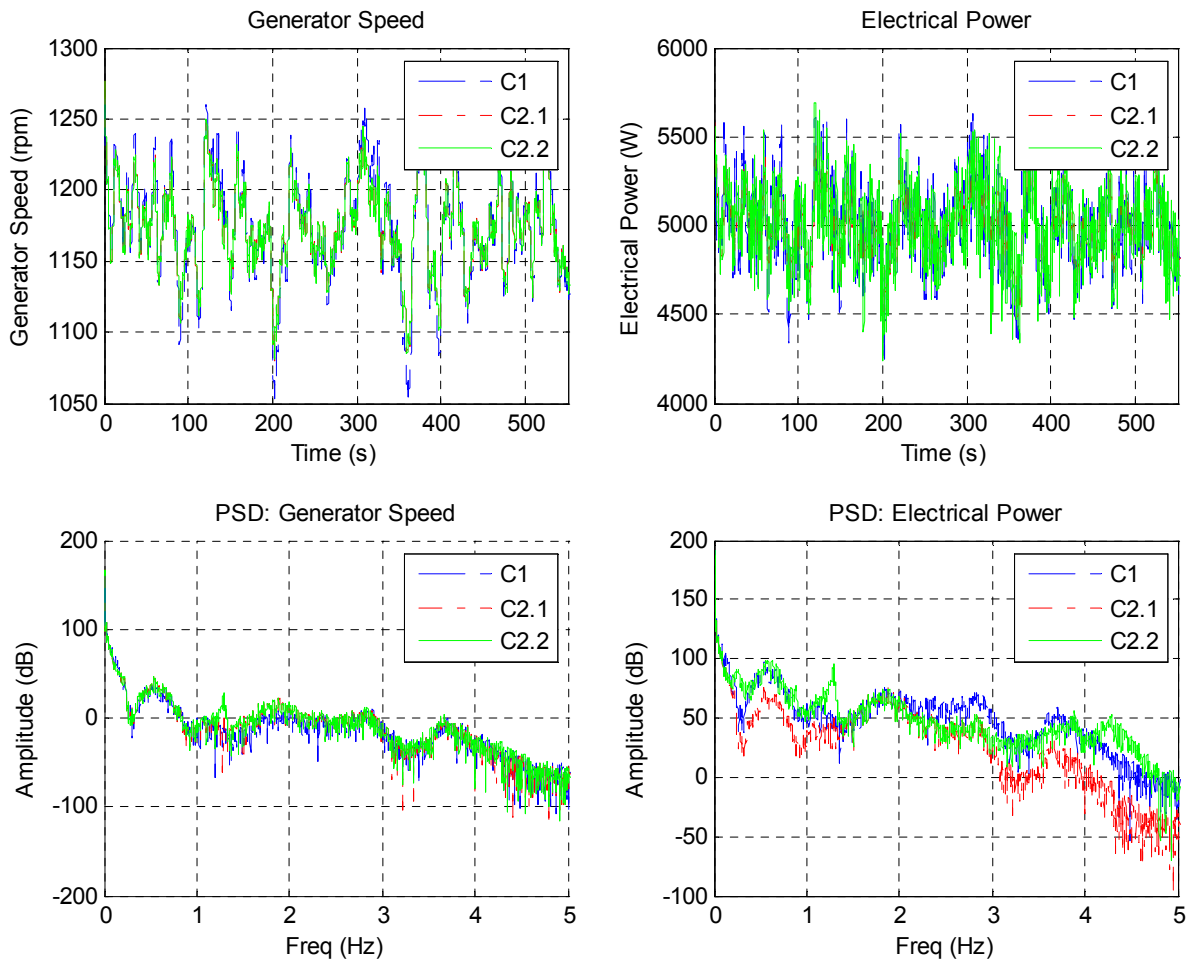
6.2. Fatigue Analysis (DLC1.2 in IEC61400-1 Second Edition)

The rain flow counting algorithm [23,24] is used to analyze the load reduction capacity of the designed controllers. A fatigue analysis is carried out using this algorithm to determine the fatigue damage on the wind turbine components. The fatigue damage analysis, called load equivalent analysis, follows these steps:

1. To carry out time domain simulations using the non-linear wind turbine model and the designed controller. Twelve simulations of 600 s have been carried out using odd production winds from mean speeds from 3 m/s to 25 m/s.
2. To subject some signals of loads in time simulations (stationary hub M_x , stationary hub M_y , tower base M_x , tower base M_y , blade M_{Flap} and blade M_{Edge}) to the rain flow counting algorithm (one for each measured variable) using the toolbox in MATLAB [25] to carry out this analysis.
3. To obtain the load equivalent L_{eq} (14) for each kind of material and for each simulated wind. The material is defined by the m value. m is the slope of the SN curve of the material, where S is the fatigue strength and N the number of cycles to failure. N_i , the number of cycles, and L_i , the cycles amplitudes, are extracted from the rainflow counting and N_{rd} is the number of points of the time domain simulation. For glass fibre $m = 10$, for cast modular iron $m = 7$ and for welded steel $m = 3$:

$$L_{eq} = \left(\frac{\sum (n_i \cdot L_i)}{N_{rd}} \right)^{\frac{1}{m}} \quad (14)$$

Figure 17. Generator speed and electrical power with a turbulent production wind of 19 m/s.



- The twelve simulations must be taken into account to calculate the total load equivalent for each material. The load equivalent referring to the Weibull distribution w_{eqm} (15) is calculated for each wind and each material. The total load equivalent for one material L_{eqw} (16) referring to the Weibull distribution is calculated with the summation of the w_{eqm} . w_c is a parameter of the Weibull distribution, $slife$ is the standard life of wind turbines (20 years) and $tsim$ is the simulated time of the considered variable in this load equivalent analysis:

$$w_{eqm} = L_{eq}^m \cdot w_c \cdot slife / tsim \tag{15}$$

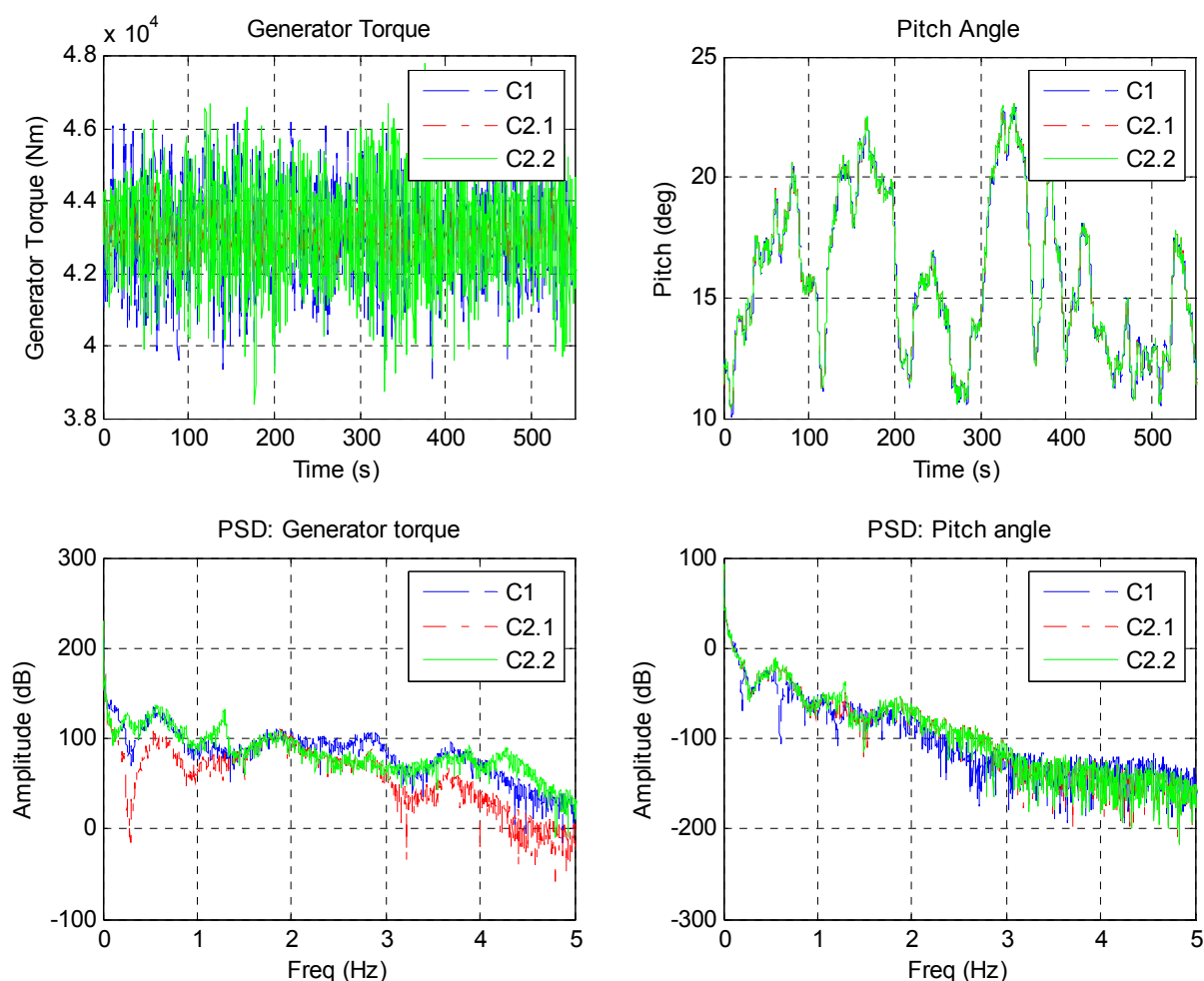
$$L_{eq} = \left(\sum w_{eqm} \right)^{(1/m)} \tag{16}$$

- To compare the wind turbine life variations $comp_{life}$ (17) between two compared load equivalent analysis. L_{eqw1} is the total load equivalent value for twelve simulations and L_{eqw2} is the other total load equivalent value for the other twelve simulations:

$$comp_{life} = \frac{slife}{\left(\frac{L_{eqw1} - L_{eqw2}}{100} \right)^m} \tag{17}$$

In Figure 17 the controlled signals (generator speed and electric power) are compared for a turbulent production wind of 19 m/s (see Figure 16) using the C1, C2.1 and C2.2 control strategies. The generator speed is controlled for the nominal value 1173 rpm and the electrical power around 5 MW. The power spectral density (PSD) performs a frequency analysis of time domain simulations. In Figure 18 the control signals (collective pitch angle and generator torque) are compared. The time domain simulation shows the quick response of the pitch angle using the C2.1 and C2.2 strategies and the torque contribution signal of the C2.2 control strategy to mitigate the side-to-side displacement on the tower. Figure 19 shows the reduction of the wind effect on the tower fore-aft mode in the tower base momentum M_y and the reduction of the wind effect on the tower side-to-side mode and drive train mode in tower base momentum M_x .

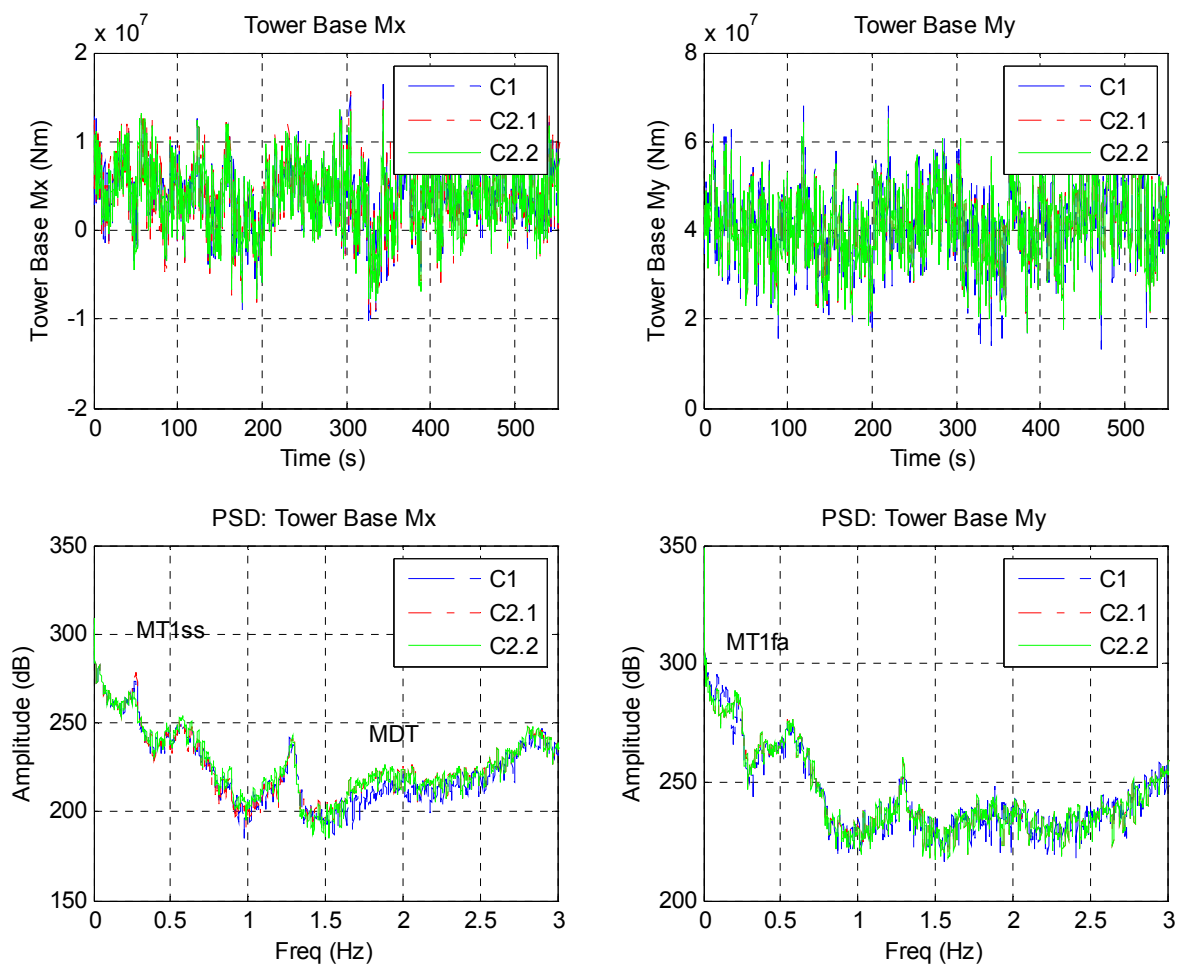
Figure 18. Generator torque and pitch angle with a turbulent production wind of 19 m/s.



Finally, the fatigue damage analysis of the components of the wind turbine is carried out as a result of the load equivalent analysis. Table 4 shows the load reduction percentage of the control strategies on the different components of the Upwind model. C1 is the reference strategy to compare the load reduction achieved with C2.1 and C2.2 control strategies. Results are calculated for three material constants, m , which are commonly used by the commercial companies of wind turbines. If $m = 3$ using the two H_∞ MISO controllers, the load reduction is 0.4% on the Stationary Hub M_x momentum using the C2.2 control strategy and 4.8% using the C2.1 strategy, 13.4% on the Tower Base M_x momentum

with the C2.2 and 2.6% using the C2.1, and 4.7% on the Tower Base My momentum respect to the C1 baseline controller using the C2.2 and 5.2% with the C2.1. If $m = 9$, the load reduction is 3.1% on the Stationary Hub Mx momentum, 19.6% on the Tower Base Mx momentum and 8.8% on the Tower Base My momentum using the C2.2 control strategy. On the other hand, if $m = 9$ using the C2.1 control strategy, the load reduction is 4.2% on the Stationary Hub Mx momentum, -0.1% on the Tower Base Mx momentum and 10.9% on the Tower Base My momentum. If $m = 12$ using the C2.2 strategy, the load reduction is 2.9% on the Stationary Hub Mx momentum, 19.2% on the Tower Base Mx momentum and 10.6% on the Tower Base My momentum. For this m value using the C2.1 control strategy, the load reduction is 4.0% on the Stationary Hub Mx momentum, -0.2% on the Tower Base Mx momentum and 13.6% on the Tower Base My momentum. Load reduction figures less than 0.4% should not be considered because they can be caused by mathematical calculation precision in the load equivalent algorithm (in blue colour in Table 4).

Figure 19. Loads on tower base with a turbulent production wind of 19 m/s.



In these simulations there is an excitation of the rotor in-plane 1st FW mode M_{R1ipfw} (1.2 Hz). This excitation is not critical from the point of view of the load reduction in a wind turbine system as proven in this load equivalent analysis. The cause of this excitation is the bandwidth of the torque controller. The torque controller reduces the wind effect on the drive train mode M_{DT} (1.6 Hz) and tower 1st side-to-side mode M_{T1ss} (0.28 Hz). The torque H_∞ MISO controller (see Figure 8) dynamics

from tower top side-to-side acceleration to torque set point value introduces a high gain in frequencies between 0.2 Hz and 1.6 Hz which produces the In plane 1st FW mode excitation. To reduce this excitation, a notch filter in the rotor in-plane 1st FW frequency must be included in the weight functions W_2 used to design the torque controller.

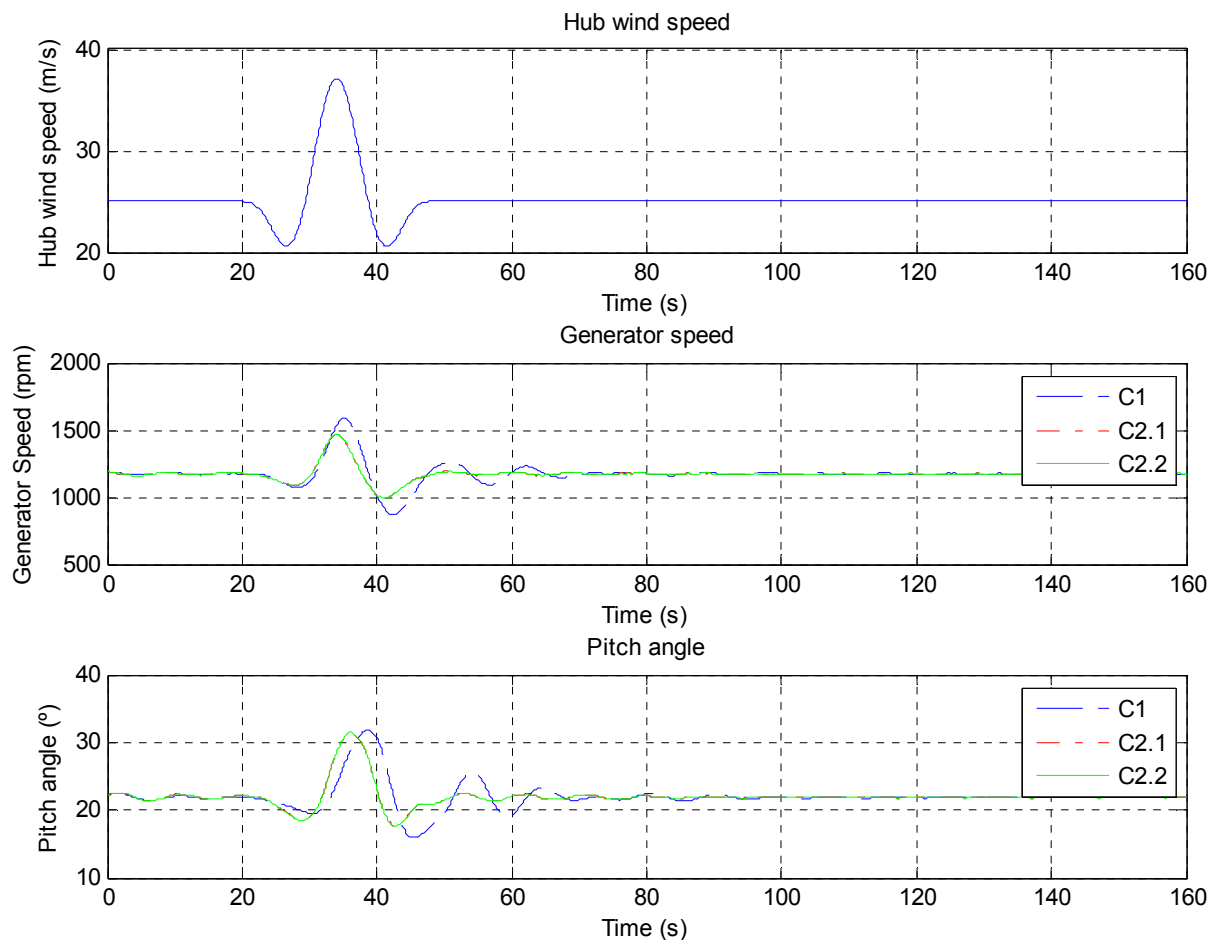
Table 4. Comparison of the load equivalent analysis.

	m	C1-C2.1 (%)	C1-C2.2 (%)
Stationary Hub Mx	3	4.8	0.4
	9	4.2	3.1
	12	4.0	2.9
Stationary Hub My	3	0.2	0.2
	9	0.9	1
	12	1.2	1.5
Gearbox Torque	3	4.8	0.4
	9	4.2	3.1
	12	4.0	2.9
Tower Base Mx	3	2.6	13.4
	9	-0.1	19.6
	12	-0.2	19.2
Tower Base My	3	5.2	4.7
	9	10.9	8.8
	12	13.6	10.6
Blade1 MFlap	3	0.1	-0.2
	9	0.1	-0.1
	12	0.1	-0.2
Blade1 MEdge	3	0	0.1
	9	0	0
	12	0	0

6.3. Extreme Load Analysis (DLC1.6 in IEC61400-1 Second Edition)

The extreme load DLC1.6 analysis studies the system response for different kinds of extreme gusts. This analysis is divided into three different steps:

1. To carry out time domain simulations using the non-linear wind turbine model and the C1 and C2 different control strategies. Six simulations of different kinds of gusts have been carried out. The gusts are called Vr-0, Vr-p, Vr-n, Vout-0, Vout-p, Vout-n.
2. To analyze the six simulations and extract the maximum value of the generator speed signal and some momentums (tower base Mx, tower base My, tower base Mxy, hub total bending Myz, blade MFlap and blade MEdge).
3. To compare these maximum values using the C2 control strategy with regard to the baseline C1 control strategy.

Figure 20. Vout-p extreme gust simulation.

Other extreme load cases (as for instance DLC1.5 in IEC61400-1 Second Edition cases) are not taken into account because results depend especially on the stop strategy, which has not been implemented. Moreover, a safety control strategy is not developed in the supervisory control to stop the wind turbine in generator over-speed cases. This article only shows the response of the developed C1 and C2 control strategies in the above rated zone without taking into account any safety control strategy.

The results of the extreme load DLC1.6 analysis are summarized in Table 5. The C2.1 and C2.2 control strategies, based on the H_{∞} norm reduction, give better results than the baseline control strategy C1. Using C2.2, the reduction of the generator speed maximum value, compared to the C1 strategy, is 7.8%, the tower base Mx momentum is reduced by 7.8% and the blade MEdge momentum is reduced by 26.3%. The tower base My momentum, tower base Mxy momentum and hub total bending Myz momentum are reduced by around 1.5% when using the C2.2 control strategy. Using C2.1, the reduction of the generator speed maximum value is 7.8%, the tower base Mx momentum is not reduced and the blade MEdge momentum is reduced by 25.9%. However, the tower base My momentum, tower base Mxy momentum and hub total bending Myz momentum are not considerably reduced using the C2.1 control strategy. The blade MEdge momentum is considerably reduced due to the increase in the generator speed output disturbance bandwidth and the reduction in the peak of this sensitivity function. In Figure 20, the results of the simulation in GH Bladed using an input of wind of

a Vout-p gust and using the C1 control strategy are compared to the same wind input using the C2 control strategy without including any safety system to avoid generator over-speeds. The higher bandwidth of the generator speed output sensitivity function obtained with the C2 control strategy means a quick response of the collective pitch angle signal and the consistent reduction of the generator speed maximum value. Furthermore, the mitigation of the variations of the generator speed using the H_∞ controllers is the main reason for the mitigation of the extreme load on the blade MEdge momentum. The most useful advantage of this reduction of extreme loads using the H_∞ control strategy is to avoid the activation of special safety strategies to stop the wind turbine. Usually, these special safety strategies are activated when the generator speed is higher than a critical value and involves losses of the electric power and critical momentary increases of loads in the wind turbine.

Table 5. Comparison of the extreme load analysis.

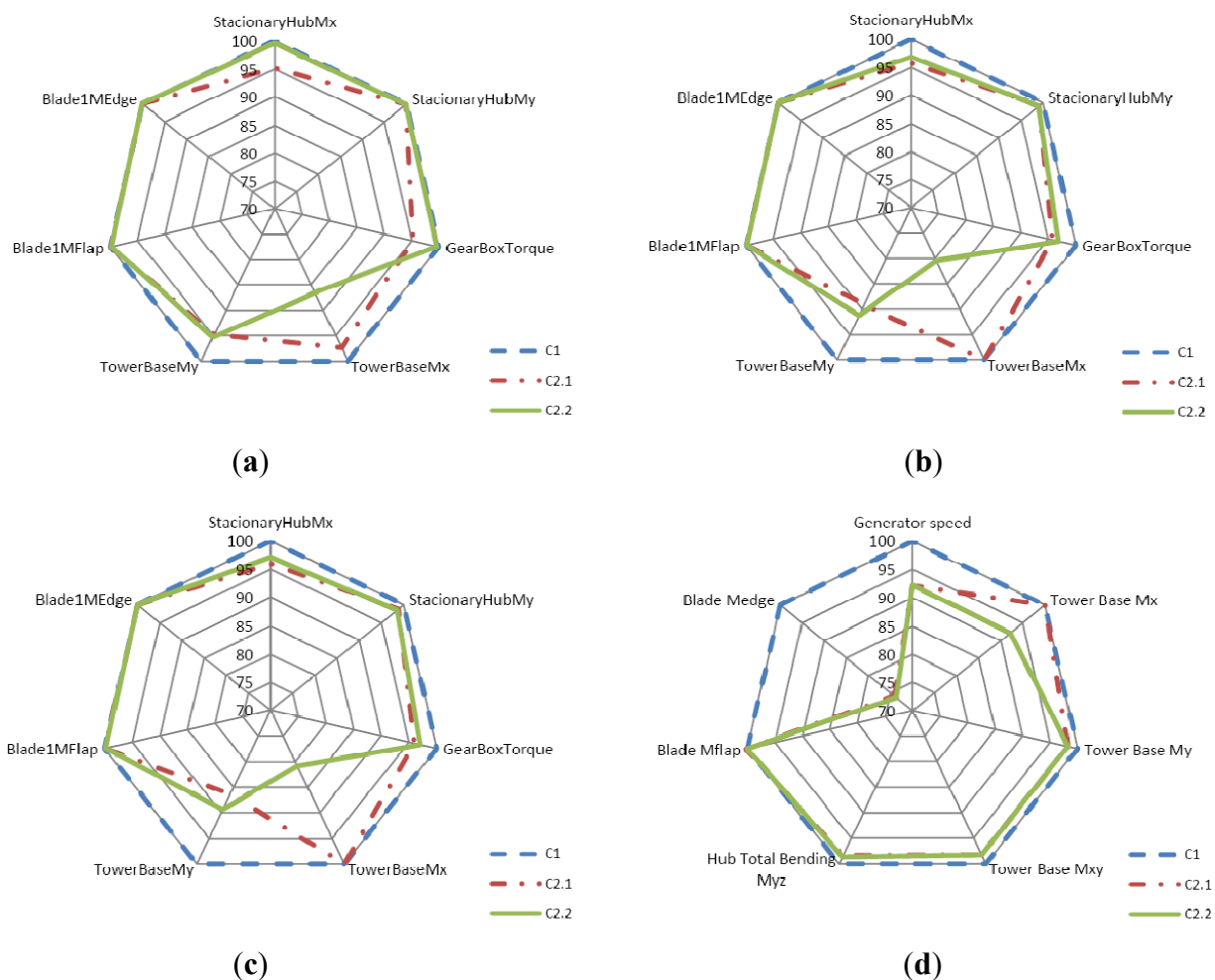
	C1	C2.1	C1-C2.1 (%)	C2.2	C1-C2.2 (%)
Generator Speed	1589 rpm	1464 rpm	7.86	1465 rpm	7.8
Tower Base Mx	29278 KNm	29285 KNm	0.02	26983 KNm	7.8
Tower Base My	158258 KNm	155500 KNm	1.74	155473 KNm	1.7
Tower Base Mxy	158311 KNm	155500 KNm	1.77	155555 KNm	1.7
Hub total bending Myz	12991 KNm	12780 KNm	1.62	12817 KNm	1.3
Blade MFlap	18341 KNm	18400 KNm	-0.32	18355 KNm	-0.07
Blade MEdge	9946 KNm	7366 KNm	25.94	7327 KNm	26.3

7. Conclusions

The work carried out and presented in this article can be summarized as follows:

1. The offshore Upwind 5 MW wind turbine model is developed using the GH Bladed 4.0 software package.
2. A classical control strategy for wind turbines is defined and it is considered the baseline controller for comparing with the new developed control strategies.
3. New design process of a control strategy based on H_∞ controllers is defined and validated in GH Bladed. The new strategies are applied in above rated power production zone in wind turbines. The results obtained in the closed loop simulations using GH Bladed 4.0 software package show the fatigue load reduction on the desired components (tower and drive train) compared to the classical baseline control strategy (see Figure 21). Using the designed H_∞ controllers, the extreme load reduction in case DLC1.6 does not appear only in the tower, but also in the three blades. Results obtained using H_∞ controllers have these outstanding benefits from the load reduction point of view due to some interesting properties:

Figure 21. Review of load mitigation (a) Equivalent load analysis $m = 3$; (b) Equivalent load analysis $m = 9$; (c) Equivalent load analysis $m = 12$; (d) Extreme load analysis.



- The attenuation of the generator speed output disturbance bandwidth is higher than that obtained using the classical control strategy.
- The attenuation of the generator speed output disturbance peak is higher than that obtained using the classical control strategy.
- The proposed control strategy based on the H_∞ norm reduction takes into account the coupling between variables in the wind turbine system. The designed controller is multivariable and multi-objective.
- The controller robustness is guaranteed due to the small gain theorem properties applied to the H_∞ controller synthesis.
- Some notch filters can be included in the controller dynamics using a correct definition of the mixed sensitivity problem. This is very useful for reducing excited modes on non-desired frequencies.

Acknowledgements

The work described in this paper has been supported in part by the Basque Country Government (Spain) and the Regional Council of Aquitaine (France), in the frame of Cooperation Commons Funds Euskadi-Aquitaine (Project Bladed).

References

1. Caselitz, P.; Geyler, M.; Giebhardt, J.; Panahandeh, B. Hardware-in-the-Loop development and testing of new pitch control algorithms. In *Proceeding of European Wind Energy Conference and Exhibition (EWEC)*, Brussels, Belgium, March 2011; pp. 14–17.
2. Johnson, K.E.; Pao, L.Y.; Balas, M.J.; Kulkarni, V.; Fingersh, L.J. Stability analysis of an adaptive torque controller for variable speed wind turbines. In *Proceeding of IEEE Conference on Decision and Control*, Atlantis, Bahamas, December 2004; pp. 14–17.
3. Nourdine, S.; Díaz de Corcuera A.; Camblong, H.; Landaluze, J.; Vechiu, I.; Tapia, G. Control of wind turbines for frequency regulation and fatigue loads reduction. In *Proceeding of 6th Dubrovnik Conference on Sustainable Development of Energy, Water and Environment Systems*, Dubrovnik, Croatia, September 2011; pp. 25–29.
4. Wright, A.D. *Modern Control Design for Flexible Wind Turbines*; NREL/TP-500-35816; Technical Report for NREL: Colorado, CO, USA, July 2004.
5. Wright, A.D.; Fingersh, L.J.; Balas, M.J. Testing state-space controls for the controls advanced research turbine. In *Proceeding of 44th AIAA Aerospace Sciences Meeting and Exhibit*, Reno, NV, USA, January 2006; pp. 9–12.
6. Sanz, M.G.; Torres, M. Aerogenerador síncrono multipolar de velocidad variable y 1.5 MW de potencia: TWT1500. *Rev. Iberoamer. Autom. Informát.* **2004**, *1*, 53–64.
7. Bianchi, F.D.; Battista, H.D.; Mantz, R.J. Wind turbine control systems. In *Principles, Modelling and Gain Scheduling Design*; Springer-Verlag: London, UK, 2007.
8. Geyler, M.; Caselitz, P. Robust multivariable pitch control design for load reduction on large wind turbines. *J. Sol. Energy Eng.* **2008**, *130*, 12.
9. Fleming, P.A.; van Wingerden, J.W.; Wright, A.D. Comparing state-space multivariable controls to multi-*siso* controls for load reduction of drivetrain-coupled modes on wind turbines through field-testing. NREL/CP-5000-53500; NREL: Colorado, CO, USA, 2011.
10. Jonkman, J.; Butterfield, S.; Musial, W.; Scott, G. *Definition of a 5 MW Reference Wind Turbine for Offshore System Development*; NREL/TP-500-38060; Technical Report for NREL: Colorado, CO, USA, February 2009.
11. Upwind Home page. Available online: <http://www.upwind.eu> (accessed on 12 December 2011).
12. Bossanyi, E.A. The design of closed loop controllers for wind turbines. *Wind Energy* **2000**, *3*, 149–163.
13. Bossanyi, E.A. Controller for 5 MW reference turbine. In *European Upwind Project Report*; Garrad Hassan & Partners Ltd.: Bristol, UK, 2009. Available online: <http://www.upwind.eu> (accessed on 12 December 2011).

14. Wright, A.D.; Fingersh, L.J. *Advanced Control Design for Wind Turbines Part I: Control Design, Implementation, and Initial Tests*; NREL/TP-500-42437; NREL: Colorado, CO, USA, 2008.
15. Bossanyi, E.A. Wind turbine control for load reduction. *Wind Energy* **2003**, *6*, 229–244.
16. Van der Hooft, E.L.; Schaak, P.; van Engelen, T.G. *Wind Turbine Control Algorithms*; DOWEC-F1W1-EH-03094/0; Technical Report for ECN: Petten, The Netherlands, 2003.
17. Wright, A.D.; Balas, M.J. Design of controls to attenuate loads in the controls advanced research turbine. *J. Sol. Energy Eng.* **2004**, *126*, 1083.
18. Hau, M. *Promising Load Estimation Methodologies for Wind Turbine Components*; Technical Report for European Upwind Project; ISET, Kassel, Germany, 2009. Available online: <http://www.upwind.eu> (accessed on 12 December 2012).
19. Bossanyi, E.A.; Ramtharan, G.; Savini, B. The importance of control in wind turbines design and loading. In *Proceedings of the 17th Mediterranean Conference on Control & Automation*, Thessaloniki, Greece, June 2009; pp. 24–26.
20. Balas, G.; Chiang, R.; Packard, A.; Safonov, M. MATLAB robust control toolbox. In *Getting Started Guide*; The MathWorks, Inc.: Natick, MA, USA, 2009.
21. Doyle, J.C.; Francis, B.A.; Tannenbaum, A.R. *Feedback Control Theory*; MacMillan: Toronto, Canada, 1992.
22. Bossanyi, E.A. *Bladed User Manual*; Garrad Hassan & Partners Ltd.: Bristol, UK, 2009.
23. Frandsen, S.T. Turbulence and Turbulence Generated Structural Loading in Wind Turbine Clusters. Ph.D. Thesis, Technical University of Denmark, Roskilde, Denmark, 2007.
24. Söker, H.; Kaufeld, N. Introducing low cycle fatigue in IEC standard range pair spectra. In *Proceeding of 7th German Wind Energy Conference*, Wilhelmshaven, Germany, October 2004; pp. 20–21.
25. MATLAB Rainflow Counting Algorithm Toolbox. Available online: <http://www.mathworks.com/MATLABcentral/fileexchange/3026> (accessed on 12 December 2011).

© 2012 by the authors; licensee MDPI, Basel, Switzerland. This article is an open access article distributed under the terms and conditions of the Creative Commons Attribution license (<http://creativecommons.org/licenses/by/3.0/>).